Research Paper

GEOSPHERE

GEOSPHERE; v. 13, no. 4

doi:10.1130/GES01459.1

3 figures; 1 supplemental file

CORRESPONDENCE: mariachiara.zaffani@studenti.unipd.it

CITATION: Zaffani, M., Agnini, C., Concheri, G., Godfrey, L., Katz, M., Maron, M., and Rigo, M., 2017, The Norian "chaotic carbon interval": New clues from the $\delta^{13}C_{org}$ record of the Lagonegro Basin (southern Italy): Geosphere, v. 13, no. 4, doi:10.1130/GES01459.1.

Received 28 November 2016
Revision received 3 March 2017
Accepted 14 April 2017

The Norian "chaotic carbon interval": New clues from the $\delta^{13}C_{org}$ record of the Lagonegro Basin (southern Italy)

Mariachiara Zaffani[1], Claudia Agnini[1,6], Giuseppe Concheri[2], Linda Godfrey[3], Miriam Katz[4], Matteo Maron[1,5], and Manuel Rigo[1,6]

[1]Department of Geosciences, University of Padova, via Gradenigo 6, 35131 Padova, Italy
[2]Department of Agronomy, Food, Natural Resources, Animals and the Environment (DAFNAE), University of Padova, Viale dell'Università 16, 35020 Legnaro (PD), Italy
[3]Department of Earth and Planetary Sciences, Rutgers University, Piscataway, New Jersey 08854, USA
[4]Department of Earth and Environmental Sciences, Rensselaer Polytechnic Institute, 110 8th St., Troy, New York 12180, USA
[5]Department of Earth Sciences "Ardito Desio," University of Milan, via Mangiagalli, 34, 20133 Milan, Italy
[6]Institute of Geosciences and Earth Resources–Consiglio Nazionale delle Ricerche (CNR), Via G. Gradenigo 6, 35131 Padova, Italy

ABSTRACT

A global carbon-isotope curve for the Late Triassic has the potential for global correlations and new insights on the complex and extreme environmental changes that took place in this time interval. We reconstruct the global $\delta^{13}C_{org}$ profile for the late Norian, improving on sparse published data from North American successions that depict a "chaotic carbon-isotope interval" with rapid oscillations. In this context, we studied three sections outcropping in the Lagonegro Basin (southern Italy), originally located in the western Tethys. The carbon-isotope profiles show four negative excursions correlatable within the Lagonegro Basin. In particular, a negative shift close to the Norian/Rhaetian boundary (NRB) appears to correlate with that observed in the North American $\delta^{13}C_{org}$ record, documenting the widespread occurrence of this carbon cycle perturbation. The $^{87}Sr/^{86}Sr$ and $^{187}Os/^{188}Os$ profiles suggest that this negative shift was possibly caused by emplacement of a large igneous province (LIP). The release of greenhouse gases (CO_2) to the atmosphere-ocean system is supported by the ^{12}C enrichment observed, as well as by the increase of atmospheric pCO_2 inferred by different models for the Norian/Rhaetian interval. The trigger of this strongly perturbed interval could thus be enhanced magmatic activity that could be ascribed to the Angayucham province (Alaska, North America), a large oceanic plateau active ca. 214 ± 7 Ma, which has an estimated volume comparable to the Wrangellia and the Central Atlantic Magmatic Province (CAMP) LIPs. In fact, these three Late Triassic igneous provinces may have caused extreme environmental and climate changes during the Late Triassic.

INTRODUCTION

The Triassic is a key period in Earth's history, characterized by breakup of the supercontinent Pangea, episodes of biotic crises, and climate fluctuations (e.g., Ogg, 2012). This period is constrained by: (1) the end-Permian mass extinction—the most extensive biotic decimation of the Phanerozoic (e.g., Lucas, 1999; Benton and Twitchett, 2003; Lucas and Orchard, 2004; Erwin, 2006); and (2) the end-Triassic mass extinction (e.g., Hallam, 2002; Tanner et al., 2004; Richoz et al., 2007). The Triassic is also characterized by a dynamic climate regime (e.g., Preto et al., 2010; Rigo et al., 2012b; Trotter et al., 2015) and widespread geological and paleontological events, including humid and warm episodes (e.g., Carnian Pluvial Event, Upper Triassic, Simms and Ruffell, 1989, 1990; Simms et al., 1995; Ruffell et al., 2015), volcanism, and changes in the biosphere (e.g., Raup and Sepkoski, 1982; McElwain et al., 1999; Hallam, 2002; Marzoli et al., 2004; McRoberts et al., 2008; Lucas, 2010; Rigo and Joachimski, 2010; Rigo et al., 2012b; Dal Corso et al., 2012, 2014; Trotter et al., 2015). Stable isotopes play a critical role in biogeochemical cycles and therefore can provide important clues of ocean-water chemistry, oxygenation, and productivity of marine environments during the Triassic. Among these tools, one of the most widely applied is $\delta^{13}C_{org}$. This isotopic system varies in time as a function of productivity, organic carbon burial, and C assimilation pathway (C3 or C4). Therefore, $\delta^{13}C_{org}$ can provide essential clues on the evolution of ocean-water chemistry, oxygenation, and productivity of past marine environments (e.g., Hayes et al., 1999; Veizer et al., 1999; Payne et al., 2004; Korte et al., 2005; Lucas, 2010; Preto et al., 2012). In particular, excursions in marine $\delta^{13}C_{org}$ records that can be correlated globally are often thought to be related to global changes in the carbon cycle, such as those induced by marine and terrestrial extinction episodes (Berner, 2002; Galli et al., 2005; Payne and Kump, 2007; Korte and Kozur, 2010), which are often marked by negative $\delta^{13}C_{org}$ anomalies.

The carbon-isotope record of the Triassic has been studied in some detail, but its interpretation is complex because of the multiple ecological and geochemical controls on this proxy (e.g., Hayes et al., 1999; Veizer et al., 1999; Muttoni et al., 2004, 2010, 2014; Payne et al., 2004; Galli et al., 2005, 2007; Korte et al., 2005; Lucas, 2010; Mazza et al., 2010; Preto et al., 2012). A pronounced negative excursion is recorded at the Permian/Triassic boundary with oscillations in the lowermost Triassic, which is characterized by strong isotopic instability (e.g., Payne et al., 2004; Lucas, 2010). This is followed by a more stable period in the Middle Triassic (Payne et al., 2004; Tanner, 2010) and early Late Triassic

(Julian, lower Carnian), with steadily rising values of $\delta^{13}C_{org}$ and $\delta^{13}C_{carb}$ likely related to environmental recovery after the Late Permian mass extinction and increasing storage of organic carbon in terrestrial environments (e.g., Lucas, 2010). The Late Triassic is bracketed by two significant negative shifts, both linked to a large igneous province (LIP). The first occurred in the Carnian and is associated with the Carnian Pluvial Event and emplacement of the Wrangellia igneous province (e.g., Furin et al., 2006; Dal Corso et al., 2012, 2015). The second is at the Triassic/Jurassic transition associated with the end-Triassic mass extinction and emplacement of the Central Atlantic Magmatic Province (CAMP) (e.g., Marzoli et al., 2004; Whiteside et al., 2010; Schaller et al., 2012; Dal Corso et al., 2014). The causes of the Triassic carbon-isotope excursions remain a topic of much debate, with the most likely trigger mechanisms being outgassing during volcanic activity, changes in productivity, ocean anoxia, and/or seafloor methane release (e.g., Richoz et al., 2007; Lucas, 2010). These processes evidently perturbed the global carbon cycle and caused episodes of biotic crises (e.g., Rampino and Stothers, 1988; Jones and Jenkyns, 2001; Wignall, 2001; Ward et al., 2004; Richoz et al., 2007; van de Schootbrugge et al., 2008; Jenkyns, 2010; Tanner, 2010; Pálfy and Kocsis, 2014, Trotter et al., 2015). Therefore, a global carbon-isotope curve for the Triassic would have the potential for global correlation and would provide new insights on the environmental changes that took place in this period. Muttoni et al. (2014) provide a composite $\delta^{13}C_{carb}$ record from the Ladinian (ca. 242 Ma) to present, but the construction of a Triassic organic carbon-isotope record is still in progress. Published $\delta^{13}C_{org}$ data are especially focused on mass extinction events (i.e., Permian/Triassic boundary and Triassic/Jurassic boundary), whereas the long-term background conditions are largely understudied. For instance, sparse carbon-isotope data are available for the Late Triassic, which seems to be characterized by significant $\delta^{13}C_{org}$ excursions associated with important episodes of faunal turnovers. In particular, data from the Norian (ca. 227.0–205.7 Ma; Diakow et al., 2011, 2012; Maron et al., 2015) of North America seem to indicate rapid oscillations of $\delta^{13}C_{org}$ that culminate in a positive $\delta^{13}C_{org}$ excursion that corresponds to the extinction of the bivalve *Monotis*, at the Norian/Rhaetian boundary (Ward et al., 2004; Wignall et al., 2007; Whiteside and Ward, 2011). This positive excursion is interpreted to have resulted from increased stagnation in ocean circulation (Sephton et al., 2002; Ward et al., 2004). Tethyan sections have been investigated for $\delta^{13}C_{carb}$ at the Norian/Rhaetian boundary (e.g., Atudorei, 1999; Gawlick and Bohm, 2000; Hauser et al., 2001; Muttoni et al., 2004, 2010; Hornung and Brandner, 2005; Korte et al., 2005; Preto et al., 2013; Bertinelli et al., 2016; Rigo et al., 2016), but the Norian organic carbon-isotope profile remains incomplete.

Therefore, the aim of this study is to verify the occurrence and to understand the causes of the Norian organic carbon-isotope perturbations in the Tethyan realm, in particular in the Lagonegro Basin (southern Italy), as a contribution to the construction of a more complete global C_{org} isotope curve for the Late Triassic. For this purpose, we investigated three geological sections, representing intermediate to distal basinal pelagic successions, for the concentration of total organic carbon (TOC) and organic carbon isotopes ($\delta^{13}C_{org}$).

GEOLOGIC SETTING

The Lagonegro Basin is located in the Southern Apennines (Italy) and is interpreted as part of the Ionian Sea, a branch of the western Tethys Ocean (Şengör et al., 1984; Catalano et al., 2001; Stampfli and Marchant, 1995; Ciarapica and Passeri, 1998, 2002; Stampfli et al., 2003). The Lagonegro Basin is interpreted as an oceanic basin based on the available seismic lines and magnetic anomaly pattern of the Ionian Sea, which show that the sedimentary succession of this area lies upon oceanic crust (e.g., Finetti, 1982; Finetti et al., 1996; Catalano et al., 2001; Argnani, 2005; Rigo et al., 2007, 2012a; Speranza et al., 2012). It consists of shallow to deep basinal pelagic successions, Permian to Miocene in age (Scandone, 1967; Rigo et al., 2005, 2012a, 2012b; Giordano et al., 2010). The Lagonegro sequence is subdivided into many tectonic units, accumulated between the Apenninic and Apulian carbonate platforms (Mostardini and Merlini, 1986) during the Apenninic orogenesis and formation of a part of the Southern Apennines chain (southern Italy). The Upper Triassic in the Lagonegro Basin is represented by the Calcari con Selce and the Scisti Silicei Formations. The Calcari con Selce consists of calcilutites bearing conodonts, radiolarians, and thin-shelled bivalves (e.g., *Halobia*), intercalated with marls, siltstones, and calcarenites (Rigo et al., 2005, 2012a; Giordano et al., 2010). Nodules and layers of chert are present throughout this unit, and limestones show varying degrees of dolomitization. The Scisti Silicei is characterized by centimeter-thick multicolored cherts, radiolarites, and often siliceous shales (Amodeo, 1999; Bertinelli et al., 2005a; Giordano et al., 2010). This formation represents the beginning of the biosiliceous sedimentation within the Lagonegro Basin, occurring from the uppermost Norian to lower Hettangian, thus the base of the Scisti Silicei is considered diachronous (Bertinelli et al., 2005a; Reggiani et al., 2005; Giordano et al., 2010, 2011; Casacci et al., 2016). The gradual passage between the Calcari con Selce and the Scisti Silicei is represented by the so-called "transitional interval" (Miconnet, 1982; Amodeo and Baumgartner, 1994; Amodeo, 1999; Bertinelli, 2003; Rigo et al., 2005, 2012a; Giordano et al., 2010). Going upward, the "transitional interval" shows a gradual decrease in carbonates in favor of clay and siliceous components. Silicification of the carbonates also increases upward (Amodeo, 1999; Rigo et al., 2005; Giordano et al., 2010). The base of this "transitional interval" is marked by a meter-thick level of red shales (Amodeo, 1999; Bertinelli et al., 2005a; Rigo et al., 2005, 2012a; Giordano et al., 2010), which is conventionally used as a regional lithomarker within the Lagonegro Basin. This red shale level approximates the base of the *Mockina bidentata* Zone (sensu Kozur and Mock, 1991), Sevatian 1 in age (ca. 216–210.5 Ma; Rigo et al., 2005, 2012a; Maron et al., 2015). The Triassic and Jurassic successions of the Lagonegro Basin (i.e., Calcari con Selce and Scisti Silicei) can be differentiated in proximal, intermediate, and distal facies (Scandone, 1967), depending on thickness of the formations and on the amount of resedimented calcarenites and calcirudites coming from the adjacent carbonate platforms. The proximal facies in the Calcari con Selce persisted from Upper Triassic to Middle Jurassic (Selli, 1962; Scandone, 1967; Bertinelli et al., 2005a; Passeri et al., 2005; Rigo et al., 2005; Giordano et al., 2010). Instead, the distal facies, which are characterized by the transition from the carbonate sedimentation of the Calcari con Selce to the siliceous deposition of Scisti Silicei, occurred with different patterns between the uppermost Triassic and the lowermost Jurassic (Scandone, 1967; Rigo et al., 2005, 2012a; Giordano et al., 2010).

The Lagonegro Basin has been investigated at three localities, where the Norian/Rhaetian interval is well documented: the Pignola-Abriola, Mount Volturino, and Madonna del Sirino sections (Fig. 1). These successions belong to the Calcari con Selce and Scisti Silicei and generally display good exposure and continuity in the field.

Pignola-Abriola Section

The Pignola-Abriola section crops out along the road between the villages of Pignola and Abriola (Potenza province, southern Italy) on the mountainside of Mount Crocetta (geographic coordinate system, datum WGS 84: 40°33′23.50″N, 15°47′1.71″E). This section spans from the upper part of the Calcari con Selce, where the Norian/Rhaetian transition is documented (Amodeo, 1999; Bazzucchi et al., 2005; Rigo et al., 2005, 2016; Tanner et al., 2006; Giordano et al., 2010), to the lowermost part of the Scisti Silicei. The Pignola-Abriola section lacks the red shales level of the "transitional interval" that conventionally marks the uppermost portion of Calcari con Selce. The basal part (from 0 to 13 m) of the Pignola-Abriola section consists of thin-bedded cherty limestones, sometimes dolomitized, shales, and rare thin layers of calcarenites with platform-derived bioclasts. The overlying 37 m consist of alternations of dark-gray shales, thin beds of limestones, and black cherty layers. This part of the section is characterized by a progressive decrease in the relative abundance of carbonates in favor of the cherty and siliceous components (Amodeo, 1999; Bazzucchi et al., 2005; Rigo et al., 2005; Tanner et al., 2006; Giordano et al., 2010). Repeated thin and well-laminated interbeds of black shales with the shaly interval across and above the NRB suggest a transient period between suboxic and/or anoxic to more oxic conditions (Casacci et al., 2016). The observed sedimentation pattern suggests that the Pignola-Abriola section belongs to the intermediate facies association (Scandone, 1967; Rigo et al., 2005; Giordano et al., 2010; Casacci et al., 2016).

The Pignola-Abriola section yields rich assemblages of conodonts and pyritized radiolarians (Bazzucchi et al., 2005; Rigo et al., 2005, 2016; Bertinelli et al., 2016), which were used to construct a biostratigraphic framework for the section (Fig. 2), following the conodont and radiolarian biozonations proposed respectively by Kozur and Mock (1991) and Carter (1993) and summarized in Rigo et al. (2016) and Bertinelli et al. (2016). The conodont alteration index (CAI) of the Pignola-Abriola specimens is ≤1.5 (Giordano et al., 2010). *Mockina zapfei* and *Mockina slovakensis* are present from the base of the section (Giordano et al., 2010). *Mockina bidentata* is recovered from ~7 m, defining the base of the *M. bidentata* Zone (Kozur and Mock, 1991; Giordano et al., 2010). The lowest occurrence (LO) of the conodont *Misikella hernsteini* marks the base of the *M. hernsteini–P. andrusovi* Zone (Kozur and Mock, 1991), at meter 21.4 (Giordano et al., 2010). *Misikella hernsteini* occurs with *Norigondolella steinbergensis* and *Parvigondolella andrusovi*. At ~32 m, the first occurrence of *M. hernsteini*/*Misikella posthernsteini* transitional form is observed. At 44.9 m, *Misikella koessenensis* and *M. posthernsteini* appear. The first appearance datum (FAD) of *M. posthernsteini* delineates the base of the Rhaetian stage and defines the base of the eponymous conodont biozone (Kozur and Mock, 1991; Giordano et al., 2010). *Misikella ultima* appears at ~54.2 m with *Misikella kovacsi*.

The radiolarians are generally pyritized and not well preserved but are still useful in allowing the recognition of two assemblage zone boundaries: the base of the *Betraccium deweveri* Assemblage Zone (Carter, 1993) at ~22 m (late Norian in age), and the base of the *Proparvicingula moniliformis* Assemblage Zone at 41 m.

Mount Volturino Section

The Mount Volturino section is located along the southern slope of Mount Volturino (geographical coordinate system, datum WGS 84: 40°24′13.46″N; 15°49′2.25″E). This succession can be ascribed to the Calcari con Selce and the Scisti Silicei. The basal part of the section is characterized by red shales ascribed to the "transitional interval" (Giordano et al., 2010, 2011). The overlying 56 m consists of cherty limestones with red shale intercalations, red cherts, radiolarites, black siliceous shales, and silicified calcarenites rich in organic matter (Giordano et al., 2010, 2011; Rigo et al., 2016). This section belongs to the intermediate facies association (Scandone, 1967; Giordano et al., 2010, 2011).

The "transitional interval" is characterized by a rich assemblage of conodonts and several pyritized radiolarians, unlike the Scisti Silicei, which provides a good assemblage of radiolarians but few conodonts (Fig. 2). The CAI of the Mount Volturino specimens is 3 (Giordano et al., 2010, 2011). *Parvigondolella lata*, *M. bidentate*, and *P. andrusovi* first occur at ~12 m. The first occurrence (FO) of *M. hernsteini*, which defines the base of the *M. hernsteini–P. andrusovi* Zone (Kozur and Mock, 1991; Giordano et al., 2010, 2011), occurs at ~18 m along with *Parvigondolella vrielyncki*. At ~39 m, *M. hernsteini*/*M. posthernsteini* transitional form (Giordano et al., 2010, 2011) first occurs. Unfortunately, radiolarians from the "transitional interval" are very poorly preserved (Giordano et al., 2010). The base of the *B. deweveri* Assemblage Zone (Carter, 1993) occurs at 41 m. The base of the *P. moniliformis* Zone occurs at 45 m, while the base of the *Globolaxtorum tozeri* Zone is at 51 m (Giordano et al., 2010, 2011). The Rhaetian/Hettangian boundary is approximately located in the upper portion of the section, within the Nevera Member of the Scisti Silicei (Fig. 2; Bertinelli, 2003).

Madonna del Sirino Section

The section of Madonna del Sirino is located on the western flank of Mount Sirino, along the trail connecting the Madonna del Brusco Sanctuary to the Madonna del Sirino Sanctuary (geographic coordinate system, datum WGS 84: 40°07′N; 15°48′E). The upper part of the Calcari con Selce and the Scisti

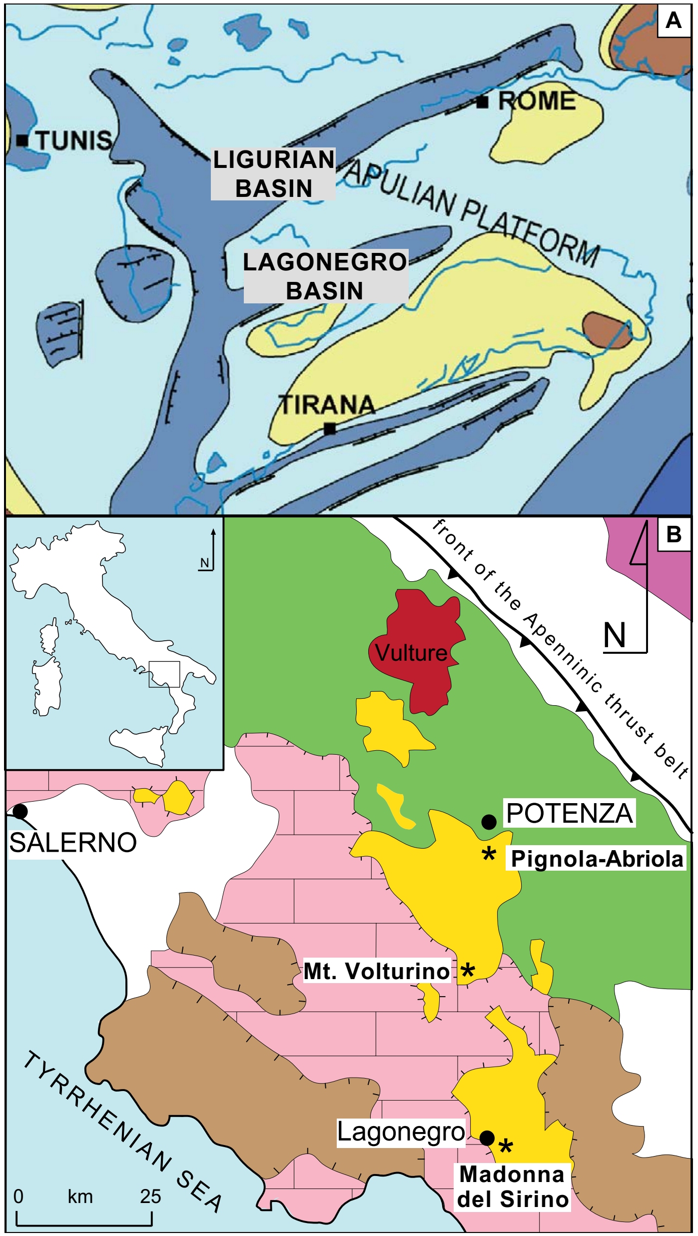

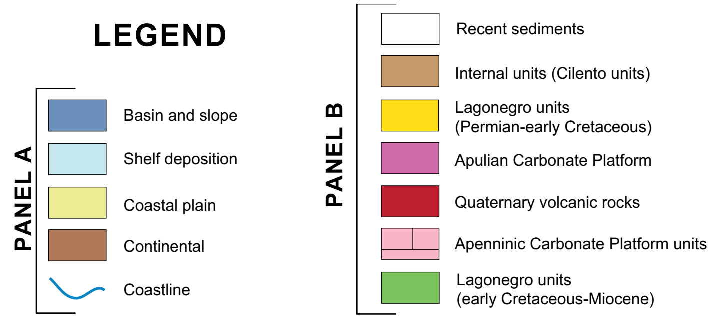

Figure 1. Paleogeography and structural map showing the tectonic units of the Lagonegro Basin. Black solid stars indicate outcrops of studied sections. Paleogeography (A) modified from Cosentino et al. (2010); structural map (B) modified from Bertinelli et al. (2005b).

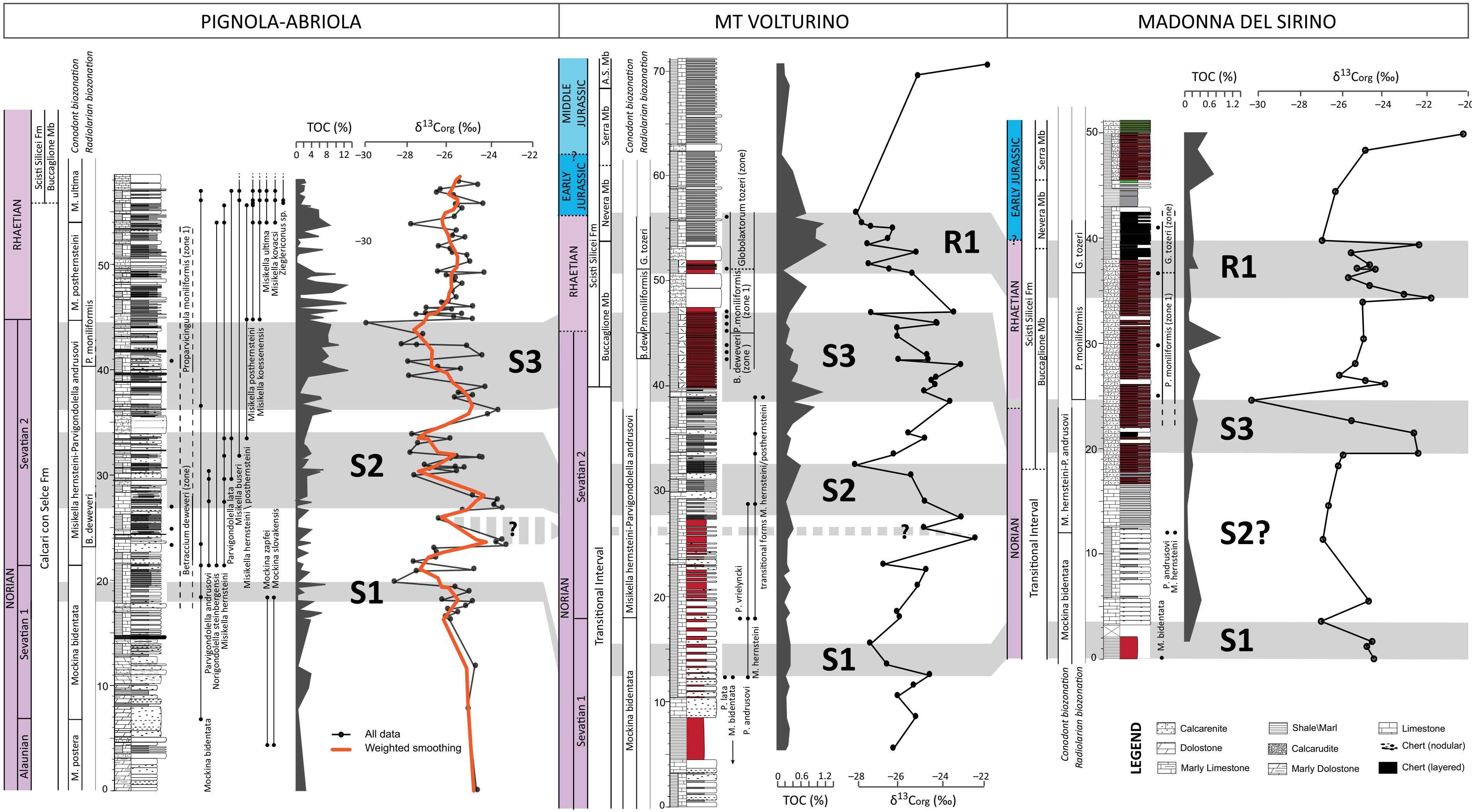

Figure 2. Lithostratigraphy, conodont and radiolarian biostratigraphy, total organic carbon (TOC), and $\delta^{13}C_{org}$ of Lagonegro sections. Biostratigraphy is based on, and integrated from, Giordano et al. (2010). Three $\delta^{13}C_{org}$ decreases (S1, S2, and S3, gray bars) are correlated using biostratigraphy. These $\delta^{13}C_{org}$ events show similar magnitude (3‰–5‰). Their durations have been established using the age model of Pignola-Abriola section provided by Maron et al. (2015): S1 = ~0.7 m.y., S2 = ~1 m.y., S3 = ~1.3 m.y. In particular, the S3 decrease culminated at the Norian/Rhaetian boundary. TOC roughly doubles within S3 at Pignola-Abriola and begins to increase by the Norian/Rhaetian boundary at the other two sections.

Silicei are exposed in this section. The Calcari con Selce consists of well-bedded micritic limestones, commonly with cherty nodules. The red horizon distinctive of the "transitional interval" lies in the upper part of Calcari con Selce exposed at this section (Reggiani et al., 2005; Tanner et al., 2007). This interval consists of siliceous shale and scattered radiolarites (Passeri et al., 2005). The overlying sediments belonging to Scisti Silicei are made up of red and green radiolarian-bearing siliceous shales and cherts with minor calcarenites (Reggiani et al., 2005; Tanner et al., 2007). The Madonna del Sirino section is characterized by small amount of platform-derived carbonates and slumps and by a reduced thickness of Scisti Silicei, thus it belongs to the distal facies association (Scandone, 1967; Miconnet, 1982; Rigo et al., 2005).

Conodont occurrences are scattered (Fig. 2), with a CAI of 3 (Reggiani et al., 2005). In contrast, radiolarians are abundant. *M. bidentata* first occurs at the base of the section, while *P. andrusovi* and *M. hernsteini* appear at ~12 m. The FO of *M. hernsteini* marks the base of the *M. hernsteini–P. andrusovi* Zone (Kozur and Mock, 1991). At ~25 m, the rich radiolarian assemblages permit the identification of the base of the *P. moniliformis* Zone (Carter, 1993). The base of the *G. tozeri* Zone occurs at ~33 m. The Rhaetian/Hettangian boundary is approximately located in the upper portion of the section, within the Nevera Member (Fig. 2), between the last occurrence of Rhaetian radiolarians and the first occurrence of Jurassic radiolarians (Reggiani et al., 2005).

METHODS

The Lagonegro Basin has been investigated for total organic carbon (TOC) content and organic carbon isotopes ($\delta^{13}C_{org}$). For the TOC analyses, we analyzed 101 rock samples from the Pignola-Abriola section, 80 samples from the Mount Volturino section, and 47 samples from the Madonna del Sirino section. For the $\delta^{13}C_{org}$ analyses, we analyzed 96 samples from the Pignola-Abriola section, 50 samples from the Mount Volturino section, and 31 samples from the Madonna del Sirino section (see Supplemental Material[1]). All samples were washed in high-purity water and selected to avoid sampling unrepresentative portions (e.g., fracture-filling mineralization, bioturbation, and diagenetic alteration). A few grams of each sample were reduced to a fine powder using a Retsch RM0 grinder and dried overnight at 40 °C.

The TOC investigations were conducted at the University of Padova. The powders were treated with a 10% HCl solution in silver capsules to remove inorganic carbon (i.e., carbonate component). Successively, they were dried on a hot plate at 50 °C and analyzed using a Vario Macro CNS Elemental Analyzer. Results were calibrated against Sulfanilamide standard (N = 16.25%; C = 41.81%; S = 18.62%; H = 4.65%). The analytical uncertainty of the instrument, expressed as relative standard deviation, is $\sigma = 0.5\%$.

For the $\delta^{13}C_{org}$ measurements, all the pulverized rock samples were acid-washed with 10% HCl for at least three hours, usually overnight. Successively, the samples were neutralized in deionized water, dried at 40 °C overnight, and wrapped in tin capsules. Forty-one samples from the Pignola-Abriola section were analyzed using a GVI Isoprime continuous-flow–isotope ratio mass spectrometer (CF-IRMS) at Rutgers University: multiple blank capsules and certified isotope standards (International Atomic Energy Agency [IAEA] N-1 = 0.43‰, IAEA N-3 = 4.72 ‰, National Bureau of Standards [NBS] 22 = –30.03‰; Coplen et al., 2006) and an in-house sediment standard were added for every batch of isotopic analysis. The standard deviation of the in-house standards during the period of analyses was better than 0.2‰. The other 60 samples from the Pignola-Abriola section and the samples from all the other sections were analyzed using a Delta V Advantage mass spectrometer connected to a Flash HT elemental analyzer at the University of Padova. For every set of analysis, multiple blank capsules and isotope standards (IAEA CH-6 = –10.45‰, IAEA CH-7 = –32.15‰, Coplen et al., 2006) were included. The standard deviation of the in-house standard during the period of analyses was better than 0.3‰.

Duration of isotopic excursions has been calculated by applying the age model proposed by Maron et al. (2015) on the Pignola-Abriola section (see Supplemental Material [see footnote 1]). This model is based on the magnetostratigraphic correlation with the Newark APTS (Maron et al., 2015).

RESULTS

We construct late Norian global $\delta^{13}C_{org}$ records for three sections outcropping in the Lagonegro Basin (southern Italy). Several lines of evidence indicate that our $\delta^{13}C_{org}$ data record a likely primary signal. First, the conodont alteration index (CAI) of specimens recovered in the Lagonegro Basin ranges between ≤1.5 (Pignola-Abriola; Giordano et al., 2010) and 3 (Mount Volturino and Madonna del Sirino; Bazzucchi et al., 2005; Reggiani et al., 2005; Rigo et al., 2005, 2012a), suggesting that the burial temperatures never exceeded 100 °C (Epstein et al., 1977; Di Leo et al., 2002) and 200 °C (Epstein et al., 1977; Bazzucchi et al., 2005; Reggiani et al., 2005; Rigo et al., 2005, 2012a), respectively. The effect of these temperatures is negligible on the $\delta^{13}C_{org}$ signal, because temperatures approaching those of oil generation are required to significantly alter the $\delta^{13}C_{org}$ primary signal (Cramer and Saltzman, 2007). Second, the Pignola-Abriola $\delta^{13}C_{org}$ trend is consistent with (and adds significant detail to) the $\delta^{13}C_{carb}$ profile illustrated in Preto et al. (2013) for the Norian/Rhaetian interval (S3 in Fig. 3).

The Pignola-Abriola $\delta^{13}C_{org}$ profile shows greater detail than the Mount Volturino and Madonna del Sirino profiles. This different resolution is mainly related to the greater abundance of organic matter in the samples (see the TOC content in Fig. 2) of the Pignola-Abriola section, which allows us greater density of $\delta^{13}C_{org}$ analyses. The samples also contain a higher siliciclastic component (i.e., dark shales and marls), and this lithological feature is likely related to the more proximal position of the Pignola-Abriola section within the Lagonegro Basin (Scandone, 1967; Amodeo, 1999; Bertinelli et al., 2005b; Rigo et al., 2005, 2016; Giordano et al., 2010, 2011).

The Pignola-Abriola $\delta^{13}C_{org}$ profile depicts three decreases (S1, S2, and S3) followed by a recovery phase toward background values (Fig. 2). Using the

TOC and $\delta^{13}C_{org}$ analyses

Sample list and results.

Pignola-Abriola

m	sample	Lithology	TOC%	$\delta^{13}C_{org}$
58.10	Pa i 191	Silicificated limestone	1.984	
57.80	Pai 189	Silicificated limestone	2.321	-25.56
57.65	GNM 119	Silicificated limestone	0.149	
57.50	Pai 187	Silicificated limestone	2.014	-24.66
57.05	Pai 185	Silicificated limestone	1.863	-26.43
56.76	GNM 117	Silicificated limestone	0.452	-26.61
56.50	Pai 184	Silicificated limestone	2.103	-25.80
55.70	GNI 29	Silicificated limestone	0.960	-24.41
55.63	Pai 180	Black shale	3.654	-25.71
55.55	GNI 28	Black shale	1.259	-25.63
55.25	GNI 27	Black shale	5.548	-25.40

[1]Supplemental Material. Sample list, total organic carbon and $\delta^{13}C_{org}$ analyses, and duration of isotopic excursions in Pignola-Abriola section (age model by Maron et al., 2015). Please visit http://doi.org/10.1130/GES01459.S1 or the full-text article on www.gsapubs.org to view the Supplemental Material.

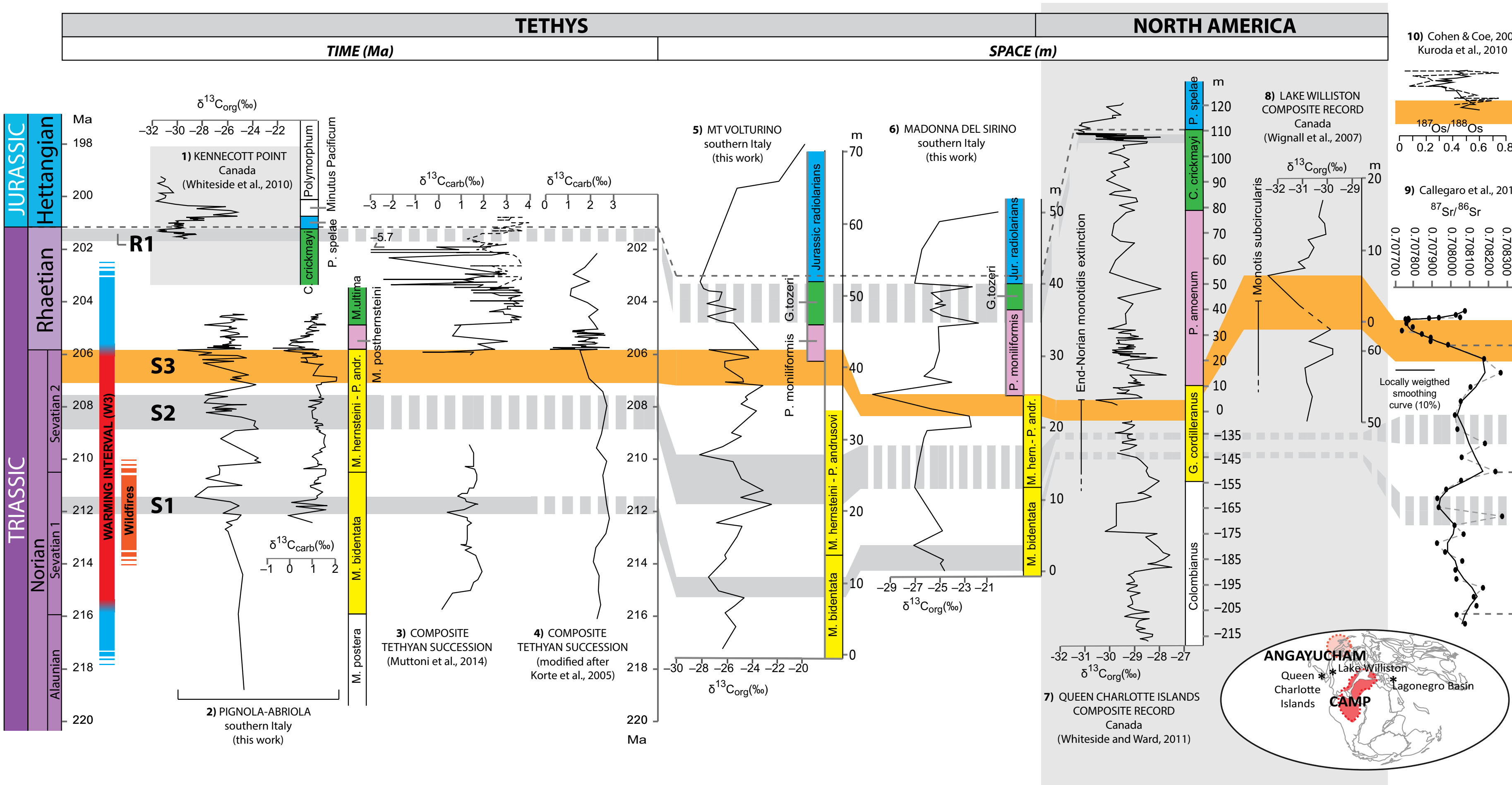

Figure 3. Correlation of the Lagonegro $\delta^{13}C_{org}$ profiles with published records: (1) Kennecott Point section, Queen Charlotte Islands, British Columbia, Canada (Hesselbo et al., 2002, then Whiteside et al., 2010); (2) $\delta^{13}C_{org}$ and $\delta^{13}C_{carb}$ of Pignola-Abriola section, Lagonegro Basin, Italy (this work, chronology by Maron et al., 2015; $\delta^{13}C_{carb}$ record modified from Preto et al., 2013); (3) composite $\delta^{13}C_{carb}$ record from Muttoni et al. (2014): Pizzo Mondello (southern Italy, from ca. 215 to ca. 209 Ma) and Brumano (northern Italy, from ca. 206 to ca. 202 Ma) and Italcementi Quarry (northern Italy, dashed line); (4) composite $\delta^{13}C_{carb}$ record from Korte et al. (2005); (5) Mount Volturino section, Lagonegro Basin, Italy (this work); (6) Madonna del Sirino section, Lagonegro Basin, Italy (this work); (7) composite profile for Queen Charlotte Islands: Kennecott Point (from 0 to 120 m) and Frederick Islands (from –215 m to –135 m) (Whiteside and Ward, 2011); (8) Lake Williston, British Columbia, Canada (Wignall et al., 2007); and (9) $^{87}Sr/^{86}Sr$ profile from Callegaro et al. (2012): data from conodonts (Callegaro et al. [2012] original data and Korte et al. [2003]). The $^{87}Sr/^{86}Sr$ profile has been smoothed using the LOcally WEighted Scatterplot Smoothing (LOWESS) method (smoothing factor = 10%). North American successions are highlighted in the light-gray boxes. $\delta^{13}C_{org}$ correlations rely on chemostratigraphy and biostratigraphy. Biostratigraphic correlations between ammonoid and conodont biozones are based on Rigo et al. (2016). The carbon-isotope stratigraphy of the Pignola-Abriola section depicts three decreases of similar magnitude (3‰–5‰) and duration (~1 m.y.) throughout the late Norian (S1, S2—highlighted by gray bars; and S3—highlighted by the orange bar). In particular, S3 appears to occur also in other Tethyan and North American successions (chemostratigraphic correlation highlighted by the orange bar). This correlation is well constrained by conodont, ammonoid, radiolarian, and bivalve biostratigraphy. S3, along with S1 and S2, correlates with the decreasing trends in the $^{87}Sr/^{86}Sr$ record (Callegaro et al., 2012). All these oscillations occur within the W3 warming interval (sensu Trotter et al., 2015; blue and red bar). Fire scars (red bar) left on petrified trunks, indicating wildfires, show similar age (Norian) (Byers et al., 2014). The Late Triassic Angayucham large igneous province (Alaska) paleogeographic position (Sussman and Weil, 2004) is shown as a red dotted circle on the map; the age of the Angayucham large igneous province (LIP) is 214 ± 7 Ma (Ernst and Buchan, 2001; Prokoph et al., 2013), compatible with the Norian carbon and strontium decreases. The late Rhaetian–early Hettangian $\delta^{13}C_{org}$ signature of the Central Atlantic Magmatic Province (CAMP) is highlighted by R1 gray bar. Its original areal extent (Marzoli et al., 1999) is shown on the map as a gray dotted area. All the discussed sections are shown on the map: (1) British Columbia Islands (Canada); (2) Lake Williston (Canada); and (3) Lagonegro Basin (Italy).

age model for the Pignola-Abriola section of Maron et al. (2015), it is possible to propose durations for these isotopic excursions.

The first $\delta^{13}C_{org}$ decrease (S1) has an amplitude of ~4‰ and occurs within the *Mockina bidentata* Zone, upper Sevatian 1. The recovery phase toward higher values is recorded above the *M. bidentata* and *M. hernsteini–P. andrusovi* Zones, in the Sevatian 2. The duration of S1 is ~0.70 m.y.

The second decrease (S2) predates the first appearance of the *M. hernsteini/posthernsteini* transitional forms (sensu Giordano et al., 2010, 2011). This negative oscillation shows an amplitude of ~4‰ and lasts for ~1.00 m.y.

The third decrease (S3) in the carbon-isotope profile culminates at the Norian/Rhaetian boundary, over the *M. hernsteini–P. andrusovi* and *M. posthernsteini* Zones and within the base of the radiolarian *P. moniliformis* Zone. This decrease reaches the lowest $\delta^{13}C_{org}$ value at the Norian/Rhaetian boundary (sensu Maron et al., 2015; Rigo et al., 2016), almost in correspondence to the FAD of the conodont *M. posthernsteini*. It shows the highest amplitude among the observed oscillations (~6‰) and lasts for ~1.33 m.y. The recovery phase occurs within the *M. posthernsteini* Zone. The return to background $\delta^{13}C_{org}$ values is associated with persistent high TOC content, a feature that is not evident in the recovery phases of S1 and S2.

Using biostratigraphy (conodont and radiolarian biozonations), we try to correlate these three $\delta^{13}C_{org}$ decreases (S1, S2, and S3) with the Mount Volturino and Madonna del Sirino $\delta^{13}C_{org}$ profiles, as shown in Figure 2. In Mount Volturino and Madonna del Sirino, a ~4‰ decrease occurs within the *Mockina bidentata* Zone (Fig. 2), which has been identified as S1. Within the *M. hernsteini–P. andrusovi* Zone, a ~4.5‰ decrease is recorded in the Mount Volturino section, which we correlate with S2. Apparently, S2 is not recorded in Madonna del Sirino, but this could be an artifact due to the low-resolution sampling and the poor biostratigraphic resolution of the section. Notably, S2 is preceded by a ~2‰ negative peak (dashed in Fig. 2) in both the Pignola-Abriola and Mount Volturino sections, supporting our correlations. However, because this negative peak is constrained by few data and is not documented in the Madonna del Sirino section, we conservatively do not use this negative peak for correlations outside the Lagonegro Basin. S3 seems easily correlatable within the Lagonegro Basin: in Mount Volturino and Madonna del Sirino, it reaches its minimum within the base of the radiolarian *P. moniliformis* Zone, depicting an amplitude of ~4‰ and 6‰, respectively (Fig. 2). Notably, in Mount Volturino and Madonna del Sirino sections, S1–S3 do not show the high-frequency fluctuations that marked the Pignola-Abriola $\delta^{13}C_{org}$ decreases (Fig. 2). These high-frequency fluctuations could be explained simply by the different sampling resolution of the study sections, but they could be also the result of a variable mixing of carbon with different isotopic composition, provenance, and source in the Pignola-Abriola section, especially if we recall that this is the most proximal site (e.g., Holmden et al., 1998; Veizer et al., 1999; Immenhauser et al., 2003; Swart and Eberli, 2005; Swart, 2008; Muttoni et al., 2014).

In the Madonna del Sirino and Mount Volturino sections, a fourth $\delta^{13}C_{org}$ decrease is recorded in the upper Rhaetian (R1, Fig.2), just below the Rhaetian/Hettangian boundary (201.3 ± 0.2; Schoene et al., 2010), within the radiolarian *G. tozeri* Assemblage Zone. The R1 $\delta^{13}C_{org}$ decrease has an amplitude of 5‰–6‰ and is not documented in the Pignola-Abriola section because this succession terminated before the Triassic/Jurassic boundary (Fig. 2).

DISCUSSION

Correlations with Published Records

The detailed comparison of the studied sections indicates that the carbon-isotope records are correlatable within the Lagonegro Basin, especially for S3, suggesting that these recurrent decreases in $\delta^{13}C_{org}$ are likely a common feature within the Basin. The correlation among the studied sections cannot be considered an artifact of the lithostratigraphy, because the base of the Scisti Silicei has been shown to be diachronous within the Basin (Giordano et al., 2010, 2011). Moreover, based on chemostratigraphy integrated with biostratigraphy, the isotopic trend appears unrelated to the lithological facies; in fact, coeval shifts are observed in different lithological units (Fig. 2).

Only a few other Norian sections have been investigated for the organic carbon-isotope record. Wignall et al. (2007) observed a ~3‰ negative $\delta^{13}C_{org}$ shift at the Norian/Rhaetian boundary in the composite Lake Williston record (British Columbia, Canada), likely correlatable with our S3 event (Fig. 3), based on biostratigraphic constraints. Specifically, the extinction of the large forms of bivalve *Monotis*, the FAD of the conodont *Misikella posthernsteini*, and the base of the radiolarian *Proparvicingula moniliformis* Zone are considered virtually coeval biohorizons (Rigo et al., 2016) and have been suggested in fact to be used to approximate the base of the Rhaetian stage (Ogg in Gradstein et al., 2012; Rigo et al., 2016; Bertinelli et al., 2016). Notably, S3 in Lake Williston is not characterized by a highly noisy record as in Pignola-Abriola (Fig. 3), where the high-frequency fluctuations are probably due, as discussed above, either to the higher sampling resolution or to mixed carbon sources.

In the Kennecott Point section (Queen Charlotte Islands, British Columbia, Canada), Ward et al. (2004) recognized a positive $\delta^{13}C_{org}$ excursion corresponding with the extinction of the bivalve *Monotis*, at the Norian/Rhaetian boundary, which is interpreted as resulting from enhanced stagnation due to subdued ocean circulation (Sephton et al., 2002; Ward et al., 2004). This result conflicts with the negative $\delta^{13}C_{org}$ shift recorded at the Norian/Rhaetian boundary in the Lagonegro Basin (Maron et al., 2015; Rigo et al., 2016; this work). In fact, Ward et al. (2004) and subsequently Whiteside and Ward (2011) establish the base of the Rhaetian stage at the last occurrence of the bivalve *Monotis*. In their work, Ward et al. (2004) noticed a reduction in maximum *Monotis* shell size approaching the final extinction. The presence of dwarfed forms has been observed also by McRoberts et al. (2008) and explained as a peculiar feature of *Monotis* around the Norian/Rhaetian boundary in response to stressed environments and/or during recovery phases following mass extinction events. Therefore, the $\delta^{13}C_{org}$ negative peak ($\delta^{13}C_{org}$ = –30.5‰) occurring ~10 m below the positive $\delta^{13}C_{org}$ excursion recorded in Kennecott Point section and coinciding with the last occurrence of the large-sized *Monotis* (i.e., ~8 cm, Ward et al., 2004) could be correlated with the minimum $\delta^{13}C_{org}$ value reached in S3 in the Lagonegro Basin (Fig. 3). Whiteside and Ward (2011) implemented the Kennecott Point $\delta^{13}C_{org}$ record with new data from Frederick Islands (Queen Charlotte Islands, British Columbia, Canada), offering an almost complete Norian organic carbon-isotope stratigraphy for the Queen Charlotte Islands. The North American Norian $\delta^{13}C_{org}$ record is characterized by rapid oscillations associated with relatively low faunal generic diversity (Whiteside and Ward, 2011). These carbon-cycle perturbations are referred to as a "chaotic carbon interval," which is in contrast to stable carbon-isotope intervals characterized by high-richness faunas (Whiteside and Ward, 2011). Using the biostratigraphic constraints proposed by Rigo et al. (2016), the conodont and radiolarian biozones recognized in the Lagonegro Basin can be correlated to the ammonoid biozones of the North America realm. Specifically, the ammonoid *Gnomohalorites cordilleranus* Zone coincides with the conodont *Mockina bidentata* Zone and *Parvigondolella andrusovi–Misikella hernsteini* Zone, while the *Paracochloceras amoenum* Zone corresponds to the conodont *M. posthernsteini* Zone and radiolarian *Proparvicingula moniliformis* Zone (Orchard, 1991; Carter, 1993; Dagys and Dagys, 1994; McRoberts et al., 2008). Therefore, we tentatively correlated S1 and S2 with the two Norian decreases recorded at Queen Charlotte Islands as shown in Figure 3. In agreement with the biostratigraphic correlations summarized in Rigo et al. (2016), S1 and S2 should occur within the base of the ammonoid *G. cordilleranus* Zone, while S3 should reach its minimum close both to the base of the ammonoid *P. amoenum* Zone and the disappearance of large forms of bivalve *Monotis*. As already discussed, a significant negative peak occurred in correspondence to the extinction of the Norian *Monotis* forms, which we correlated to the S3 minimum. According to this correlation, the observed $\delta^{13}C$ perturbations can be traced over wide areas (i.e., North America and Tethys domains): in fact, the Lagonegro Basin was located on the eastern side of the supercontinent Pangea, while the Queen Charlotte Islands were positioned on the other side of the Panthalassa Ocean during the Norian (Fig. 3). These results consequently suggest a global significance of the $\delta^{13}C$ perturbations and, in turn, of the mechanisms affecting the organic carbon record during the late Norian.

Causes of Carbon-Cycle Perturbations

The multiple $\delta^{13}C_{org}$ events documented in the Norian were likely caused by retention of ^{12}C or the release of isotopically light carbon into the atmosphere-ocean system. This relative increase in ^{12}C can originate from different mechanisms, such as the isolation of an epeiric sea, a decrease in primary productivity, or input of ^{12}C from a comet impact, methane hydrate dissociation, peatland thermal decomposition, and/or enhanced magmatic activity (e.g., Kent et al., 2003; Hesselbo et al., 2004; Higgins and Schrag, 2006; Jenkyns, 2010; Tanner, 2010; Meyers, 2014; Schaller et al., 2016). S1 and S2 are recognizable at least at a basinal level, while S3 seems to have a more convincing global occurrence (Rigo et al., 2016). Therefore, since S1–S2 and S3, are likely different in nature, different causative mechanisms should be invoked to explain these perturbations in the $\delta^{13}C_{org}$ curve.

S1 and S2 require some local mechanism(s) affecting the Lagonegro Basin during the late Norian. These two decreases might be explained as the result of changes in relative contributions of $\delta^{13}C_{org}$ components. Organic matter present in sediments can include a number of different components, such as bacteria, phytoplankton, zooplankton, pollen, and/or other terrestrial biomass. Each of these components is characterized by a specific value of $\delta^{13}C_{org}$. This means that changes in relative contributions of these components could affect the bulk $\delta^{13}C_{org}$ record, without necessarily requiring changes in the global isotope composition of the ocean and/or the atmosphere (van de Schootbrugge et al., 2008; Fio et al., 2010; Bartolini et al., 2012), which instead would be reflected as global $\delta^{13}C_{org}$ variations.

The interpretation of S3 requires a more comprehensive discussion. Because this $\delta^{13}C_{org}$ decrease has been clearly recognized on both sides of the supercontinent Pangea, we should consider only those mechanisms able to affect the global carbon cycle. Therefore, we can exclude some of the above-listed hypotheses. First, it is well established that the Lagonegro Basin was a branch of the western Tethys, not an epeiric sea (Şengör et al., 1984; Catalano et al., 2001; Stampfli et al., 1991; Stampfli and Marchant, 1995; Ciarapica and Passeri, 1998, 2002; Stampfli et al., 1998; Stampfli et al., 2003; Speranza et al., 2012). Second, the decrease in primary productivity, as explanation for $\delta^{13}C_{org}$ decrease, should result in a TOC decrease; instead, TOC maintains almost constant values throughout the Lagonegro Basin record and even increases in the Pignola-Abriola S3, where it roughly doubles (Fig. 2). Third, a comet impact can release ~10^2 to 10^3 Gt of light carbon ($\delta^{13}C = -45‰$) depending on its size (Greenberg, 1998), producing a rapid (less than 1 k.y.) negative shift in the $\delta^{13}C$ values of ~0.2‰–1.6‰ (Kent et al., 2003; Kaiho et al., 2009). A comet impact is thus able to cause sudden and short-lived decreases in the $\delta^{13}C$ record, which contrasts with the gradual and relatively slow decreases over S3 of the studied $\delta^{13}C_{org}$ profiles. Moreover, the only impact structure crater documented in the upper Norian is the Manicougan crater, which has a radiometric age of ca. 214.5 (214.5 ± 0.5 Ma with $^{40}Ar/^{39}Ar$ and 214.56 ± 0.05 Ma with U/Pb dating, Ramezani et al., 2005), ~3 m.y. before S1.

Among the remaining hypotheses, the most plausible mechanism able to introduce isotopically light carbon into the atmosphere-ocean system throughout the latest Norian could be the injection of volcanogenic greenhouse gases. The Rhaetian $\delta^{13}C_{org}$ decrease (R1) might instead be correlated with the negative organic carbon-isotope excursion recognized worldwide just before the Triassic/Jurassic boundary, the so-called initial negative carbon-isotope excursion (CIE) (McElwain et al., 1999; Pálfy et al., 2001, 2007; Hesselbo et al., 2002; Dal Corso et al., 2014). The initial CIE is proposed as a prelude phase of the main CAMP activity (e.g., Hesselbo et al., 2002; Guex et al., 2004; Whiteside et al., 2010; Ruhl and Kurschner, 2011; Dal Corso et al., 2014). If this is true, the Norian organic carbon-isotope perturbations recorded in the Lagonegro Basin could be interpreted as pulsed pre-CAMP volcanic activity, and S3 might have been caused by a separate input of volcanogenic CO_2 to the atmosphere-ocean system. We cannot exclude a priori that S1 and S2 also might be the result of inputs of volcanogenic CO_2. In fact, the recurrent $\delta^{13}C_{org}$ decreases (S1, S2, and S3) during the Norian could be interpreted as representing the typical pulsing behavior of magmatic activity (e.g., Tolan et al., 1989; Saunders et al., 1997; Courtillot and Renne, 2003; Jerram and Widdowson, 2005; Ernst et al., 2008; Greene et al., 2012). We cannot exclude that S1 and S2 might occur at global scale, but we were not able to recognize them in the North American Lake Williston section because this succession covers a limited interval across only the Norian/Rhaetian boundary $\delta^{13}C_{org}$. Moreover, the correlation with the composite British Columbia Islands succession is not straightforward because of a gap immediately below the Norian/Rhaetian boundary. Nevertheless, in order to take into consideration on one hand results and on the other hand the reliability of proposed correlations, the following interpretations can be considered more pertinent for S3 and hypothetical for S1 and S2.

These volcanic emissions would have enhanced chemical weathering via acceleration of the hydrological cycle and increased nutrient discharge (e.g., nitrates and phosphates) to the ocean, driving increased biological productivity (e.g., Jones and Jenkyns, 2001; Jenkyns, 2010; Pogge von Strandmann et al., 2013) and resulting in high TOC content, which is observed in the case of the Pignola-Abriola S3 event.

These recurrent inputs of isotopically light carbon are recorded also in the Norian/Rhaetian composite $\delta^{13}C_{carb}$ profile constructed by Muttoni et al. (2014) (Fig. 3). This composite $\delta^{13}C_{carb}$ curve depicts three negative peaks at ca. 212, 206, and 202 Ma, correlatable with the dating of the minimum $\delta^{13}C_{org}$ values of S1, S3, and R1 respectively (ca. 211.5, 206, and 201 Ma; Fig. 3). Unfortunately, this $\delta^{13}C_{carb}$ curve (Muttoni et al., 2014) has a gap exactly in the interval between 209 and 207 Ma, when S2 may have occurred. To further support the global significance of S3, we also compare our data with the $\delta^{13}C_{carb}$ profile of Korte et al. (2005), which displays a minimum value of the $\delta^{13}C_{carb}$ at ca. 206 Ma, correlatable with the S3 negative $\delta^{13}C_{org}$ peak at Pignola-Abriola (Fig. 3). This line of evidence further highlights the global meaning of the Norian/Rhaetian boundary carbon-cycle perturbation (i.e., S3).

The occurrence of Norian volcanic activity is also supported by an increase of surface water temperature of the Tethyan subtropics of ~6 °C (~1.5‰), recorded in the $\delta^{18}O_{phos}$ curve from biogenic apatite (labeled "W3" in Trotter et al., 2015). The W3 warming phase is documented in the Norian and is correlatable with S1, S2, and S3 $\delta^{13}C_{org}$ decreases (Fig. 3). A late Norian warming is further supported by paleobotanical and pedogenic evidence, which estimate an increase of atmospheric CO_2 from 600 to 2100–2400 ppm and 2000–3000 ppm, corresponding to a warming of ~3–4 °C and 7–10 °C, respectively (McElwain et al., 1999; Cleveland et al., 2008). The proposed scenario is hence in agreement with estimates based on numerical coupled ocean-atmospheric climate models performed for the Upper Triassic (Huynh and Poulsen, 2005).

An additional piece of evidence supporting the hypothesis of a magmatic activity as the source of isotopically light carbon in the system is the $^{87}Sr/^{86}Sr$ record (Callegaro et al., 2012). Because the residence time of strontium is longer (~2.4 m.y.; Jones and Jenkyns, 2001) than the mixing time of the ocean (~1–2 k.y.; e.g., Broecker and Li, 1970; Gordon, 1973; Hodell et al., 1990; Garrett and St. Laurent, 2002), the $^{87}Sr/^{86}Sr$ curve is representative of the global seawater composition (Veizer et al., 1997; Korte et al., 2003). The $^{87}Sr/^{86}Sr$ composition of seawater is controlled by two major fluxes: the riverine flux, whose $^{87}Sr/^{86}Sr$ depends on the balance between the weathering of highly radiogenic old sialic crust and less radiogenic young basalts (average $^{87}Sr/^{86}Sr$ = ~0.710) and the hydrothermal flux, sourced from the mantle ^{86}Sr (average $^{87}Sr/^{86}Sr$ = ~0.703; e.g., Faure, 1986; Palmer and Edmond, 1989; Veizer et al., 1997; Taylor and Lasaga, 1999). Therefore, increases of seawater $^{87}Sr/^{86}Sr$ are commonly interpreted as increased continental weathering of highly radiogenic old sialic crust and/or denudation rates, which in turn could be driven by humid climate and/or tectonics (Palmer and Elderfield, 1985; Raymo et al., 1988; Hodell et al., 1989), whereas negative shifts are usually linked to weathering of young basalts (which implies the emplacement of some kind of volcanic activity) and/or increased rate of seafloor spreading (Berner and Rye, 1992; Jones and Jenkyns, 2001). The $^{87}Sr/^{86}Sr$ profile (Callegaro et al., 2012) depicts three negative excursions correlatable with the $\delta^{13}C_{org}$ decreases recognized throughout the late Norian in the Lagonegro Basin, Queen Charlotte Islands and Lake Williston sections (Fig. 3). However, at the base of the Rhaetian stage, the $^{87}Sr/^{86}Sr$ curve shows an opposite trend compared to the $\delta^{13}C_{org}$ record. In fact, while the $\delta^{13}C_{org}$ returns to background values, the $^{87}Sr/^{86}Sr$ profile keeps decreasing, suggesting two possible scenarios: (1) a lag in response time of the $^{87}Sr/^{86}Sr$ system due to its longer seawater residence time; or (2) persistent magmatic activity and/or weathering of volcanic rocks, coupled with increase of primary productivity and/or inhibition of the organic matter oxidation processes (increasing $\delta^{13}C_{org}$). The decrease in efficiency of organic matter recycling mechanisms may be related to oxygen-depleted conditions, which is supported by the high TOC content (Fig. 2, see TOC content after S3 in Pignola-Abriola). Moreover, the Rhaetian $\delta^{13}C_{org}$ profile is mimicked by the $^{187}Os/^{188}Os$ curve recorded in Japan (Kuroda et al., 2010) and in the United Kingdom (Cohen and Coe, 2007), suggesting that an abrupt and intense large-scale event affected multiple isotopic systems during the Late Triassic, causing large perturbations in the $\delta^{13}C_{org}$, $\delta^{13}C_{carb}$, $^{87}Sr/^{86}Sr$, and $^{187}Os/^{188}Os$ records. Seawater $^{187}Os/^{188}Os$, like $^{87}Sr/^{86}Sr$, is controlled by two major fluxes: (1) weathering of continental crust (average $^{188}Os/^{187}Os$ = ~1.3) and (2) mantle and/or extraterrestrial inputs (average $^{188}Os/^{187}Os$ = ~0.13) (e.g., Shirey and Walker, 1998; Peucker-Ehrenbrink and Ravizza, 2000; Cohen and Coe, 2007; Kuroda et al., 2010). In particular, young mantle-derived basalts could release large amounts of unradiogenic Os; hence, based on this rationale, Os isotopes are used to identify the initiation of major basalt volcanism (e.g., Cohen and Coe, 2007; Ravizza and Peucker-Ehrenbrink, 2003; Turgeon and Creaser, 2008; Tejada et al., 2009; Kuroda et al., 2010).

The late Norian volcanic activity seems to resemble the best known Mesozoic LIPs, such as the Wrangellia (estimated duration: late Ladinian–early Norian, U-Pb zircon dating from a gabbro sill: 232.2 ± 1.0 Ma, Mortensen and

Hulbert, 1991), the CAMP (estimated duration: late Rhaetian–early Hettangian, U-Pb zircon dating of the North Mountain basalt: 201.56 ± 0.01/0.22 Ma, e.g., Marzoli et al., 2006a, 2006b; Blackburn et al., 2013), and the Karoo-Ferrar (Toarcian, 183.1 Ma, e.g., Bomfleur et al., 2014; Sell et al., 2014). The emplacement of all these LIPs coincides with episodes of significant biotic crises, suggesting that a causal relationship might exist between eruptions and climate change (e.g., Rampino and Stothers, 1988; Furin et al., 2006; Rigo et al., 2007, 2012a; Rigo and Joachimski, 2010). With respect to the tempo, the estimated duration of the Norian activity is very similar to those inferred for the CAMP and the Wrangellia. The main phase of CAMP volcanism lasted less than 1.6–2 m.y.; a comparable duration of 2 m.y. has been proposed for the Wrangellia phase (Greene et al., 2010, 2012). These durations are consistent with those estimated in the Pignola-Abriola section, where the $\delta^{13}C_{org}$ decreases last between 0.7 and 1.3 m.y. The total duration of the late Norian volcanic activity, from S1 to S3, is ~7 m.y., if the age model of Maron et al. (2015) is adopted; this is consistent with the total duration of the Karoo-Ferrar event (~8–10 m.y.; Jourdan et al., 2007; Hastie et al., 2014) and of each major pulse of the Karoo-Ferrar LIP, which lasts from ~0.8–3 to 4.5 m.y. (Jourdan et al., 2007). All these estimated durations are comparable to those observed in the Pignola-Abriola section during the late Norian (~1.3 m.y. for each decrease).

The sparse and rare outcrops of Norian successions limit the recognition of volcanic deposits associated with the emplacement of a LIP during the late Norian, which is identifiable so far only by its geochemical signatures. Volcanic deposits linked to this event could have undergone subduction, accretion as allochthonous terranes, or collision. Recent dating of the Late Triassic Angayucham large igneous province (Alaska, Pallister et al., 1989) gives an estimated age of 214 ± 7 Ma (Ernst and Buchan, 2001; Prokoph et al., 2013), which is consistent with both the Norian age of the $^{87}Sr/^{86}Sr$ and $\delta^{13}C_{org}$ decreases (from ca. 214–206 Ma, Maron et al., 2015) and distinguishable from those of Wrangellia (late Ladinian–early Norian, Mortensen and Hulbert, 1991) and CAMP activities (late Rhaetian–early Hettangian, e.g., Marzoli et al., 2006a, 2006b; Blackburn et al., 2013). The total volume of the Angayucham oceanic plateau has been evaluated from the areal extent of outcropping ophiolites, and the most recent estimates range between 225 and 450 × 10^3 km^3 (Ernst and Buchan, 2001; Prokoph et al., 2013). This volume is not dissimilar from that of the Wrangellia oceanic plateau (~500–1000 × 10^3 km^3; Lassiter et al., 1995; Ernst and Buchan, 2001; Prokoph et al., 2013), although it is one order of magnitude smaller than the volume estimated for the CAMP deposits (~2500 × 10^3 km^3) and the Karoo-Ferrar continental flood basalts (~5000 × 10^3 km^3) (Prokoph et al., 2013; Ernst and Buchan, 2001). Considering the magnitude of S3, ~3850 Gt of volcanogenic CO_2 ($\delta^{13}C$ = –5‰; e.g., Dunkley-Jones et al., 2010; Jones et al., 2015) are required to produce a ~6‰ $\delta^{13}C_{org}$ shift (e.g., Leavitt, 1982; Caldeira and Rampino, 1990; Cervantes and Wallace, 2003; Courtillot and Renne, 2003; Self et al., 2005; Beerling et al., 2007; Sobolev et al., 2011; Jones et al., 2015). If we assume that the average CO_2 emission of a large igneous province is ~0.5 wt% of the total erupted material (e.g., Leavitt, 1982; Caldeira and Rampino, 1990; Symonds et al., 1994; Cervantes and Wallace, 2003; Schminke, 2004), then the Angayucham could have introduced in the ocean-atmosphere system ~700–1750 Gt of carbon, which equals ~2560–6400 Gt of CO_2. From this calculation, it results that the carbon-dioxide emissions of a LIP of the size of the Angayucham could justify a $\delta^{13}C_{org}$ decrease such as S3.

Even if LIPs are assumed to outgas SO_2 and CO_2 at significant rates (e.g., the CAMP is thought to outgas SO_2 and CO_2 at rates of at most 1 Gt per year; Self et al., 2005), CO_2 emissions alone may not be sufficient to account for the significant magnitude of the Norian LIP $\delta^{13}C_{org}$ decreases (e.g., even up to 6‰ for Pignola-Abriola S3, this work). Therefore, some other mechanism(s) might further contribute to the effects of the late Norian LIP emissions on the carbon-isotope system. For instance, fire scars left on fossil tree trunks from the Petrified Forest Member of the Upper Triassic Chinle Formation (Arizona, United States) provide evidence of widespread peatland fires throughout the Norian and likely throughout the whole Late Triassic (Byers et al., 2014). The age of these wildfires ranges from 213.1 to 209 Ma (Ramezani et al., 2011; Byers et al., 2014), within the estimated duration of the Norian LIP activity ("Wildfires" in Fig. 3). The carbon isotopic composition of land-plant organic matter can reach values up to ~–35‰ (e.g., Meyers, 2014). As a consequence, these wildfires could play a role in explaining the large magnitude of the Norian $\delta^{13}C_{org}$ decreases. To produce a $\delta^{13}C$ shift of the magnitude of S3, these wildfires would have had to introduce ~150 Gt of carbon in the atmosphere, which corresponds to ~550 Gt of carbon dioxide. Recent studies highlight frequent wildfires during the Late Triassic, even before the above-cited interval of time (e.g., 227.6 ± 0.08 and 211.9 ± 0.7 Ma; Tanner and Lucas, 2016).

Finally, the intense warming indicated by the oxygen-isotopic record (Trotter et al., 2015), which could have occurred due to the emplacement of a Norian LIP with its associated CO_2 flux (see different CO_2 models above), might have destabilized methane hydrate reservoirs ($\delta^{13}C$ = –60‰), which could have further increased the amplitude of the observed carbon-isotope excursions. This mechanism has already been proposed to explain short-term changes during the Karoo-Ferrar carbon-isotope excursion (Kemp et al., 2005). Therefore, wildfires and clathrate dissociation may account for the minor negative peaks, the high-frequency fluctuations, and the total amplitude of changes recognized in the $\delta^{13}C_{org}$ profiles with higher resolution data sets (Fig. 3). Considering the extremely low isotopic carbon composition of clathrates (e.g., Dickens et al., 1995; Kvenvolden, 2002), ~87 Gt of carbon, i.e., ~117 Gt of methane, would be required to produce a $\delta^{13}C_{org}$ decrease such as S3. It is also worth noting that the estimated durations for the secondary and short-lived $\delta^{13}C_{org}$ peaks in the Pignola-Abriola section range between ~10 and 100 k.y. according to the age model of Maron et al. (2015), which essentially means that each single peak might represent an input of ^{12}C-rich carbon in the ocean-atmosphere system due to a combination of possible sources, which include volcanogenic gases, methane release, and wildfires. Whereas wildfires and methane hydrate dissociation contributed to the magnitude of the Norian $\delta^{13}C_{org}$ decreases, they should be considered as possible amplification factors of the magmatic activity, which we propose as the trigger mechanism of the Norian carbon-cycle perturbations.

CONCLUSIONS

The organic carbon-isotope record of the Lagonegro Basin (western Tethys) shows the occurrence of a ~5‰ negative shift close to the Norian/Rhaetian transition, preceded by two additional $\delta^{13}C_{org}$ decreases of similar magnitude (3‰–5‰), correlatable within the Lagonegro Basin. Moreover, the carbon-isotope perturbation close to the Norian/Rhaetian boundary is correlatable (using biostratigraphy) with that recognized in the North America realm, supporting the idea that the latest Norian carbon cycle was affected at a global scale. We propose that the trigger mechanism for the input of isotopically light carbon in the ocean-atmosphere system was the emplacement of a large igneous province, possibly amplified by consequent feedbacks. The $\delta^{18}O_{phos}$ profile, the $^{87}Sr/^{86}Sr$ curve, and increase in the pCO_2 values strongly support this scenario. This suggested late Norian volcanic activity was thought to be active between 214 and 206 Ma and is tentatively attributed to the Angayucham province, a complex ocean plateau originally located on the western margin of North America and today outcropping in Alaska. The late Norian $\delta^{13}C_{org}$ records presented here improve the Late Triassic organic carbon-isotope record, which displays a series of decreases we link to the emplacement of different LIPs: the late Ladinian–early Norian Wrangellia, (possibly) the late Norian Angayucham, and the late Rhaetian–early Hettangian CAMP. These events may have had extreme environmental consequences, such as a decrease in primary productivity and/or a warming phase, which could have favored the establishment of humid conditions and episodes of seawater oxygen depletion, biotic crises, and extinctions, contributing to the complex history of this particular period of time.

ACKNOWLEDGMENTS

This study was supported by the grant EX60% 60A05-7013/15 to Manuel Rigo and by the University of Padova, grants CPDA152211/15 (P.I. Manuel Rigo) and CPDA121100/12 (P.I. Nereo Preto). Stable-isotope analyses were supported by National Science Foundation grant EAR-0844252 to Linda Godfrey. Acknowledgment is made to the donors of the American Chemical Society Petroleum Research Fund for partial support of this research to Miriam E. Katz (grant 49637-DN18). We thank the editors, Prof. Lawrence Tanner, the anonymous reviewer, and the associate editor—Prof. Rhawn Dennison—for their constructive comments on the manuscript.

REFERENCES CITED

Amodeo, F., 1999, Il Triassico terminale–Giurassico del Bacino Lagonegrese: Studi stratigrafici sugli Scisti Silicei della Basilicata (Italia meridionale): Lausanne, Memoires de Geologie, v. 33, p. 1–123.

Amodeo, F., and Baumgartner, P.O., 1994, Stratigraphic revision of the Scisti Silicei Formation (Upper Triassic–Upper Jurassic), Lagonegro Basin, southern Italy: Preliminary report: Paleopelagos, v. 4, p. 35–46.

Argnani, A., 2005, Possible record of a Triassic ocean in the Southern Apennines: Bollettino della Società Geologica Italiana, v. 124, p. 109–121.

Atudorei, N.V., 1999, Constraints on the Upper Permian to Upper Triassic marine carbon isotope curve. Case studies from the Tethys [Ph.D. thesis]: Lausanne, Switzerland, Lausanne University, p. 155.

Bartolini, A., Guex, J., Spangenberg, J.E., Schoene, B., Taylor, D.G., Schaltegger, U., and Atudorei, V., 2012, Disentangling the Hettangian carbon isotope record: Implications for the aftermath of the end-Triassic mass extinction: Geochemistry, Geophysics, Geosystems, v. 13, Q01007, doi:10.1029/2011GC003807.

Bazzucchi, P., Bertinelli, A., Ciarapica, G., Marcucci, M., Passeri, L., Rigo, M., and Roghi, G., 2005, The Late Triassic–Jurassic stratigraphic succession of Pignola (Lagonegro-Molise Basin, Southern Apennines, Italy): Bollettino della Società Geologica Italiana, v. 124, p. 143–153.

Beerling, D.J., Harfoot, M., Lomax, B., and Pyle, J.A., 2007, The stability of the stratospheric ozone layer during the end-Permian eruption of the Siberian Traps: Philosophical Transactions of the Royal Society A: v. 365, p. 1843–1866, doi:10.1098/rsta.2007.2046.

Benton, M.J., and Twitchett, R.J., 2003, How to kill (almost) all life: The end-Permian extinction event: Trends in Ecology & Evolution, v. 18, p. 358–365, doi:10.1016/S0169-5347(03)00093-4.

Berner, R.A., 2002, Examination of hypotheses for the Permo-Triassic boundary extinction by carbon cycle modeling: Proceedings of the National Academy of Sciences of the United States of America, v. 99, 7, p. 4172–4177, doi:10.1073/pnas.032095199.

Berner, R.A., and Rye, D.M., 1992, Calculation of the Phanerozoic strontium isotope record of the oceans from a carbon cycle model: American Journal of Science, v. 292, p. 136–148, doi:10.2475/ajs.292.2.136.

Bertinelli, A., 2003, Il Bacino Lagonegrese-Molisano nel contesto della Tetide occidentale durante il Triassico superiore-Giurassico [Ph.D. thesis]: Perugia, Italy, Università degli Studi di Perugia, 215 p.

Bertinelli, A., Ciarapica, G., and Passeri, L., 2005a, Late Triassic–Jurassic basinal successions in Molise and northern Basilicata: The northernmost witness of the Lagonegro domain: Bollettino della Società Geologica Italiana, v. 124, p. 177–188.

Bertinelli, A., Ciarapica, G., De Zanche, V., Marcucci, M., Mietto, P., Passeri, L., Rigo, M., and Roghi, G., 2005b, Stratigraphic evolution of the Triassic–Jurassic Sasso di Castalda succession (Lagonegro basin, Southern Apennines, Italy): Bollettino della Società Geologica Italiana, v. 124, p. 161–175.

Bertinelli, A., Casacci, M., Concheri, G., Gattolin, G., Godfrey, L., Katz, M.E., Maron, M., Mazza, M., Mietto, P., Muttoni, G., Rigo, M., Sprovieri, M., Stellin, F., and Zaffani, M., 2016, The Norian/Rhaetian boundary interval at Pignola-Abriola section (southern Apennines, Italy) as a GSSP candidate for the Rhaetian stage: An update: Albertiana, v. 43, p. 6–19.

Blackburn, T.J., Olsen, P.E., Bowring, S.A., McLean, N.M., Kent, D.V., Puffer, J., McHone, G., Rasbury, E.T., and Et-Touhami, M., 2013, Zircon U-Pb Geochronology Links the End-Triassic Extinction with the Central Atlantic Magmatic Province: Science, v. 340, p. 941, doi:10.1126/science.1234204.

Bomfleur, B., Schöner, R., Schneider, J.W., Viereck, L., Kerp, H., and McKellar, J.L., 2014, From the Transantarctic Basin to the Ferrar Large Igneous Province: New palynostratigraphic age constraints for Triassic–Jurassic sedimentation and magmatism in East Antarctica: Review of Palaeobotany and Palynology, v. 207, p. 18–37, doi:10.1016/j.revpalbo.2014.04.002.

Broecker, W.S., and Li, Y.H., 1970, Interchange of water between the major oceans: Journal of Geophysical Research, v. 75, p. 3545–3552, doi:10.1029/JC075i018p03545.

Byers, B.A., Ash, S.R., Chaney, D., and DeSoto, L., 2014, First known fire scar on a fossil tree trunk provides evidence of Late Triassic wildfire: Palaeogeography, Palaeoclimatology, Palaeoecology, v. 411, p. 180–187, doi:10.1016/j.palaeo.2014.06.009.

Caldeira, K., and Rampino, M.R., 1990, Carbon dioxide emission from Deccan volcanism and a K/T boundary greenhouse effect: Geophysical Research Letters, v. 17, no. 9, p. 1299–1302, doi:10.1029/GL017i009p01299.

Callegaro, S., Rigo, M., Chiaradia, M., and Marzoli, A., 2012, Latest Triassic marine Sr isotopic variations, possible causes and implications: Terra Nova, v. 24, p. 130–135, doi:10.1111/j.1365-3121.2011.01046.x.

Carter, E.S., 1993, Biochronology and Paleontology of uppermost Triassic (Rhaetian) radiolarians, Queen Charlotte Islands, British Columbia, Canada: Lausanne, Switzerland, Memoires de Geologie, v. 11, p. 1–176.

Casacci, M., Bertinelli, A., Algeo, T.J., and Rigo, M., 2016, Carbonate to biosilica transition at the Norian–Rhaetian boundary controlled by rift-related subsidence in the western Tethyan Lagonegro Basin (southern Italy): Palaeogeography, Palaeoclimatology, Palaeoecology, doi:10.1016/j.palaeo.2016.05.007.

Catalano, R., Doglioni, C., and Merlini, S., 2001, On the Mesozoic Ionian basin: Geophysical Journal International, v. 144, p. 49–64, doi:10.1046/j.0956-540X.2000.01287.x.

Cervantes, P., and Wallace, P.J., 2003, Role of HO in subduction-zone magmatism: New insights from melt inclusions in high-Mg basalts from central Mexico: Geology, v. 31, p. 235–238, doi:10.1130/0091-7613(2003)031<0235:ROHOIS>2.0.CO;2.

Ciarapica, G., and Passeri, L., 1998, Evoluzione paleogeografica degli Appennini: Atti Tic Sc. Terra, v. 40, p. 233–290.
Ciarapica, G., and Passeri, L., 2002, The palaeogeographic duplicity of the Apennines: Bollettino della Società Geologica Italiana, v. 121, p. 67–75.
Cleveland, D.M., Nordt, L.C., Dworkin, S.I., and Atchley, S.C., 2008, Pedogenic carbonate isotopes as evidence for extreme climatic events preceding the Triassic–Jurassic boundary: Implications for the biotic crisis?: Geological Society of America Bulletin, v. 120, p. 1408–1415, doi:10.1130/B26332.1.
Cohen, A.S., and Coe, A.L., 2007, The impact of the Central Atlantic Magmatic Province on climate and on the Sr- and Os-isotope evolution of seawater: Palaeogeography, Palaeoclimatology, Palaeoecology, v. 244, p. 374–390, doi:10.1016/j.palaeo.2006.06.036.
Coplen, T.B., Brand, W.A., Gehre, M., Groning, M., Meijer, H.A.J., Toman, B., and Verkouteren, R.M., 2006, New guidelines for $\delta^{13}C$ measures: Analytical Chemistry, v. 78, p. 2439–2441, doi:10.1021/ac052027c.
Cosentino, D., Cipollari, P., Marsili, P., and Scrocca, D., 2010, Geology of the central Apennines: A regional review, in Beltrando, M., Peccerillo, A., Mattei, M., Conticelli, S., and Doglioni, C., eds., The Geology of Italy: Tectonics and Life along Plate Margins: Journal of the Virtual Explorer, v. 36, doi:10.3809/jvirtex.2010.00223.
Courtillot, V.E., and Renne, P.R., 2003, On the ages of flood basalt events: Comptes Rendus Geoscience, v. 335, p. 113–140, doi:10.1016/S1631-0713(03)00006-3.
Cramer, B.D., and Saltzman, M.R., 2007, Early Silurian paired $\delta^{13}C_{carb}$ and $\delta^{13}C_{org}$ analyses from the Midcontinent of North America: Implications for paleoceanography and paleoclimate: Palaeogeography, Palaeoclimatology, Palaeoecology, v. 256, p. 195–203, doi:10.1016/j.palaeo.2007.02.032.
Dagys, A.S., and Dagys, A.A., 1994, Global correlation of the terminal Triassic, *in* Guex, J., and Baud, A., eds., Recent Developments on Triassic Stratigraphy: Memoires de Geologie, Lausanne, v. 22, p. 25–34.
Dal Corso, J., Mietto, P., Newton, R.J., Pancost, R.D., Preto, N., Roghi, G., and Wignall, P.B., 2012, Discovery of a major negative $\delta^{13}C$ spike in the Carnian (Late Triassic) linked to the eruption of Wrangellia flood basalts: Geology, v. 40, p. 79–82, doi:10.1130/G32473.1.
Dal Corso, J., Marzoli, A., Tateo, F., Jenkyns, H.C., Bertrand, H., Youbi, N., Mahmoudi, A., Font, E., Buratti, N., and Cirilli, S., 2014, The dawn of CAMP volcanism and its bearing on the end-Triassic carbon cycle disruption: Journal of the Geological Society of London, v. 171, p. 153–164, doi:10.1144/jgs2013-063.
Dal Corso, J., Gianolla, P., Newton, R.J., Franceschi, M., Roghi, G., Caggiati, M., Raucsik, B., Budai, T., Haas, J., and Preto, N., 2015, Carbon isotope records reveal synchronicity between carbon cycle perturbation and the “Carnian Pluvial Event” in the Tethys realm (Late Triassic): Global and Planetary Change, v. 127, p. 79–90, doi:10.1016/j.gloplacha.2015.01.013.
Di Leo, P., Dinelli, E., Mongelli, G., and Schiattarella, M., 2002, Geology and geochemistry of Jurassic pelagic sediments, Scisti Silicei Formation, southern Apennines: Italy, Sedimentary Geology, v. 150, p. 229–246, doi:10.1016/S0037-0738(01)00181-6.
Diakow, L., Orchard, M.J., and Friedman, R., 2011, Absolute ages for the Norian Stage: A contribution from southern British Columbia, Canada: Canadian Paleontology Conference, Proceedings no. 9, p. 27–28.
Diakow, L., Orchard, M.J., and Friedman, R., 2012, Absolute ages for the Norian Stage: A further contribution from southern British Columbia, Canada: Cordilleran Tectonics Workshop: Geological Association Canada, Pacific Section, Program and Abstracts, 2 p.
Dickens, G.R., O’Neil, J.R., Rea, D.K., and Owen, R.M., 1995, Dissociation of oceanic methane hydrate as a cause of the carbon isotope excursion at the end of the Paleocene: Paleoceanography, v. 10, no. 6, p. 965–971, doi:10.1029/95PA02087.
Dunkley-Jones, T., Ridgwell, A., Lunt, D.J., Maslin, M.A., Schmidt, D.N., and Valdes, P.J., 2010, A Palaeogene perspective on climate sensitivity and methane hydrate instability: Philosophical Transactions of the Royal Society A, v. 368, p. 2395–2415, doi:10.1098/rsta.2010.0053.
Ernst, R.E., and Buchan, K.L., 2001, Large mafic magmatic events through time and links to mantle-plume heads, *in* Ernst, R.E., and Buchan, K.L., eds., Mantle Plumes: Their Identification through Time: Geological Society of America Special Paper 352, p. 483–575.
Ernst, R.E., Wingate, M.T.D., Buchan, K.L., and Li, Z.X., 2008, Global record of 1600–700 Ma Large Igneous Provinces (LIPs): Implications for the reconstruction of the proposed Nuna (Columbia) and Rodinia supercontinents: Precambrian Research, v. 160, p. 159–178, doi:10.1016/j.precamres.2007.04.019.
Epstein, A.G., Epstein, J.B., and Harris, L.D., 1977, Conodont color alteration: An index to organic metamorphism: U.S. Geological Survey Professional Paper 995, 27 p.
Erwin, D.H., 2006, Extinction: How Life on Earth Nearly Ended 250 Million Years Ago: Princeton, New Jersey, Princeton University Press.
Faure, G., 1986, Principles of Isotope Geology: Second edition: New York, John Wiley and Sons, p. 589.
Finetti, I., 1982, Structure, stratigraphy and evolution of central Mediterranean: Bollettino di Geofisica Teorica ed Applicata, v. 24, p. 247–315.
Finetti, I., Lentini, F., Carbone, S., Catalano, S., and Del Ben, A., 1996, Il sistema Appennino Meridionale-Arco Calabro-Sicilia nel Mediterraneo Centrale: Studio geologico-geofisico: Bollettino della Società Geologica Italiana, v. 115, p. 529–559.
Fio, K., Spangenberg, J.E., Vlahovic, I., Sremac, J., Velic, I., and Mrinjek, E., 2010, Stable isotope and trace element stratigraphy across the Permian-Triassic transition: A redefinition of the boundary in the Velebit Mountain, Croatia: Chemical Geology, v. 278, p. 38–57, doi:10.1016/j.chemgeo.2010.09.001.
Furin, S., Preto, N., Rigo, M., Roghi, G., Gianolla, P., Crowley, J.L., and Bowring, S.A., 2006, High precision U-Pb zircon age from the Triassic of Italy: Implications for the Triassic time scale and the Carnian origin of calcareous nannoplankton and dinosaurs: Geology, v. 34, p. 1009–1012, doi:10.1130/G22967A.1.
Galli, M.T., Jadoul, F., Bernasconi, S.M., and Weissert, H., 2005, Anomalies in global carbon cycling at the Triassic/Jurassic boundary: Evidence from a marine C-isotope record: Palaeogeography, Palaeoclimatology, Palaeoecology, v. 216, p. 203–214, doi:10.1016/j.palaeo.2004.11.009.
Galli, M.T., Jadoul, F., Bernasconi, S.M., Cirilli, S., and Weissert, H., 2007, Stratigraphy and palaeoenvironmental analysis of the Triassic–Jurassic transition in the western Southern Alps (Northern Italy): Palaeogeography, Palaeoclimatology, Palaeoecology, v. 244, p. 52–70, doi:10.1016/j.palaeo.2006.06.023.
Garrett, C., and St. Laurent, L., 2002, Aspects of deep ocean mixing: Journal of Oceanography, v. 58, p. 11–24, doi:10.1023/A:1015816515476.
Gawlick, H.J., and Bohm, F., 2000, Sequence and isotope stratigraphy of Late Triassic distal periplatform limestones from the Northern Calcareous Alps (Kälberstein Quarry, Berchtesgaden Hallstatt Zone): International Journal of Earth Sciences, v. 89, p. 108–129, doi:10.1007/s005310050320.
Giordano, N., Rigo, M., Ciarapica, G., and Bertinelli, A., 2010, New biostratigraphical constraints for the Norian/Rhaetian boundary: Data from Lagonegro Basin, Southern Apennines, Italy: Lethaia, v. 43, p. 573–586, doi:10.1111/j.1502-3931.2010.00219.x.
Giordano, N., Ciarapica, G., Bertinelli, A., and Rigo, M., 2011, The Norian–Rhaetian interval in two sections of the Lagonegro area: The transition from carbonate to siliceous deposition: Italian Journal of Geosciences, v. 130, p. 380–393.
Gordon, A.L., 1973, Physical oceanography: Antarctic Journal of the United States, v. 8, p. 61–69.
Gradstein, F.M., Ogg, J.G., Schmitz, M.D., and Ogg, G.M., eds., 2012, The Geological Time Scale 2012: Amsterdam, Elsevier, 2 vols., 1144 p.
Greenberg, J.M., 1998, Making a comet nucleus: Astronomy and Astrophysics, v. 330, p. 375–380.
Greene, S.E., Bottjer, D.J., Corsetti, F.A., Berelson, W.M., and Zonneveld, J.P., 2010, Might ocean acidification leave a diagenetic record?: Geological Society of America Abstracts with Programs, v. 42, no. 5, p. 437.
Greene, S.E., Martindale, R.C., Ritterbush, K.A., Bottjer, D.J., Corsetti, F.A., and Berelson, W.M., 2012, Recognizing ocean acidification in deep time: An evaluation of the evidence for acidification across the Triassic–Jurassic boundary: Earth-Science Reviews, v. 113, p. 72–93, doi:10.1016/j.earscirev.2012.03.009.
Guex, J., Bartolini, A., Atudorei, V., and Taylor, D., 2004, High-resolution ammonite and carbon isotope stratigraphy across the Triassic–Jurassic boundary at New York Canyon (Nevada): Earth and Planetary Science Letters, v. 225, p. 29–41, doi:10.1016/j.epsl.2004.06.006.
Hallam, A., 2002, How catastrophic was the end-Triassic mass extinction?: Lethaia, v. 35, p. 147–157, doi:10.1080/002411602320184006.
Hastie, W.W., Watkeys, M.K., and Aubourg, C., 2014, Magma flow in dyke swarms of the Karoo LIP: Implications for the mantle plume hypothesis: Gondwana Research, v. 25, p. 736–755, doi:10.1016/j.gr.2013.08.010.
Hauser, M., Martini, R., Burns, S., Dumitrica, P., Krystyn, L., Matter, A., Peters, T., and Zaninetti, L., 2001, Triassic stratigraphic evolution of the Arabian–Greater India embayment of the southern Tethys margin: Eclogae Geologicae Helvetiae, v. 94, p. 29–62.
Hayes, J.M., Strauss, H., and Kaufman, A.J., 1999, The abundance of ^{13}C in marine organic matter and isotopic fractionation in the global biogeochemical cycle of carbon during the past 800 Ma: Chemical Geology, v. 161, p. 103–125, doi:10.1016/S0009-2541(99)00083-2.

Hesselbo, S.P., Robinson, S.A., Surlyk, F., and Piasecki, S., 2002, Terrestrial and marine extinction at the Triassic–Jurassic boundary synchronized with major carbon-cycle perturbation: A link to initiation of massive volcanism?: Geology, v. 30, p. 251–254, doi:10.1130/0091-7613(2002)030<0251:TAMEAT>2.0.CO;2.

Hesselbo, S.P., Robinson, S.A., and Surlyk, F., 2004, Sea-level change and facies development across potential Triassic–Jurassic boundary horizons, SW Britain: Journal of the Geological Society, v. 161, p. 365–379, doi:10.1144/0016-764903-033.

Higgins, J.A., and Schrag, D.P., 2006, Beyond methane: Towards a theory for the Paleocene–Eocene thermal maximum: Earth and Planetary Science Letters, v. 245, p. 523–537, doi:10.1016/j.epsl.2006.03.009.

Hodell, D.A., Mueller, P.A., McKenzie, J.A., and Mead, G., 1989, Strontium isotope stratigraphy and geochemistry of the late Neogene ocean: Earth and Planetary Science Letters, v. 92, no. 2, p. 165–178, doi:10.1016/0012-821X(89)90044-7.

Hodell, D.A., Mead, G., and Mueller, P.A., 1990, Variation in the strontium isotopic composition of seawater (8 Ma to present): Implications for chemical weathering rates and dissolved fluxes to the oceans: Chemical Geology, v. 80, no. 4, p. 291–307, doi:10.1016/0168-9622(90)90011-Z.

Holmden, C., Creaser, R.A., Muehlenbachs, K., Leslie, S.A., and Bergstrom, S.M., 1998, Isotopic evidence for geochemical decoupling between ancient epeiric seas and bordering oceans: Implications for secular curves: Geology, v. 26, p. 567–570, doi:10.1130/0091-7613(1998)026<0567:IEFGDB>2.3.CO;2.

Hornung, T., and Brandner, R., 2005, Biochronostratigraphy of the Reingraben Turnover (Hallstatt Facies Belt): Local black shale events controlled by regional tectonics, climatic change and plate tectonics: Facies, v. 51, p. 460–479, doi:10.1007/s10347-005-0061-x.

Huynh, T.T., and Poulsen, C.J., 2005, Rising atmospheric CO_2 as a possible trigger for the end-Triassic mass extinction: Palaeogeography, Palaeoclimatology, Palaeoecology, v. 217, p. 223–242, doi:10.1016/j.palaeo.2004.12.004.

Immenhauser, A., Della Porta, G., Kenter, J.A.M., and Bahamonde, J.R., 2003, An alternative model for positive shifts in shallow-marine carbonate $\delta^{13}C$ and $\delta^{18}O$: Sedimentology, v. 50, p. 953–959, doi:10.1046/j.1365-3091.2003.00590.x.

Jenkyns, H.C., 2010, Geochemistry of oceanic anoxic events: Geochemistry, Geophysics, Geosystems, v. 11, Q03004, doi:10.1029/2009GC002788.

Jerram, D.A., and Widdowson, M., 2005, The anatomy of continental flood basalt provinces: Geological constraints on the processes and products of flood volcanism: Lithos, v. 79, p. 385–405, doi:10.1016/j.lithos.2004.09.009.

Jones, C.E., and Jenkyns, H.C., 2001, Seawater strontium isotopes, oceanic anoxic events, and seafloor hydrothermal activity in the Jurassic and Cretaceous: American Journal of Science, v. 301, p. 112–149, doi:10.2475/ajs.301.2.112.

Jones, M.T., Jerram, D.A., Svensen, H.H., and Grove, C., 2015, The effects of large igneous provinces on the global carbon and sulphur cycles: Palaeogeography, Palaeoclimatology, Palaeoecology, v. 114, p. 1–18, doi:10.1016/j.palaeo.2015.06.042.

Jourdan, F., Féraud, G., Bertrand, H., Watkeys, M.K., and Renne, P.R., 2007, Distinct brief major events in the Karoo large igneous province clarified by new $^{40}Ar/^{39}Ar$ ages on the Lesotho basalts: Lithos, v. 98, p. 195–209, doi:10.1016/j.lithos.2007.03.002.

Kemp, D.B., Coe, A.L., Cohen, A.S., and Schwark, L., 2005, Astronomical pacing of methane release in the early Jurassic period: Nature, v. 437, p. 396–399, doi:10.1038/nature04037.

Kent, D.V., Cramer, B.S., Lanci, L., Wang, D., Wright, J.D., and Van der Voo, R., 2003, A case for a comet impact trigger for the Paleocene/Eocene thermal maximum and carbon isotope excursion: Earth and Planetary Science Letters, v. 211, p. 13–26, doi:10.1016/S0012-821X(03)00188-2.

Kaiho, K., Chen, Z.Q., and Sawada, K., 2009, Possible causes for a negative shift in the stable carbon isotope ratio before, during and after the end-Permian mass extinction in Meishan, South China: Australian Journal of Earth Sciences, v. 56, p. 799–808, doi:10.1080/08120090903002615.

Korte, C., and Kozur, H.W., 2010, Carbon isotope stratigraphy across the Permian–Triassic boundary: A review: Journal of Asian Earth Sciences, v. 39, p. 215–235, doi:10.1016/j.jseaes.2010.01.005.

Korte, C., Kozur, H.W., Bruckschen, P., and Veizer, J., 2003, Strontium isotope evolution of Late Permian and Triassic seawater: Geochimica et Cosmochimica Acta, v. 67, p. 47–62, doi:10.1016/S0016-7037(02)01035-9.

Korte, C., Kozur, H.W., and Veizer, J., 2005, ^{13}C and ^{18}O values of Triassic brachiopods and carbonate rocks as proxies for coeval seawater and palaeotemperature: Palaeogeography, Palaeoclimatology, Palaeoecology, v. 226, p. 287–306, doi:10.1016/j.palaeo.2005.05.018.

Kozur, H., and Mock, R., 1991, New Middle Carnian and Rhaetian conodonts from Hungary and the Alps, stratigraphic importance and tectonic implications for the Buda Mountains and adjacent areas: Jahrbuch der Geologischen Bundesanstalt, v. 134, p. 271–297.

Kuroda, J., Hori, R.S., Suzuki, K., Grocke, D.R., and Ohkouchi, N., 2010, Marine osmium isotope record across the Triassic–Jurassic boundary from a Pacific pelagic site: Geology, v. 38, p. 1095–1098, doi:10.1130/G31223.1.

Kvenvolden, K.A., 2002, Methane hydrate in the global organic carbon cycle: Terra Nova, v. 14, p. 302–306, doi:10.1046/j.1365-3121.2002.00414.x.

Lassiter, J.C., DePaolo, D.J., and Mahoney, J.J., 1995, Geochemistry of the Wrangellia flood basalt province: Implications for the role of continental and oceanic lithosphere in flood basalt genesis: Journal of Petrology, v 36, p. 983–1009, doi:10.1093/petrology/36.4.983.

Leavitt, S.W., 1982, Annual volcanic carbon dioxide emission: An estimate from eruption chronologies: Environmental Geology v. 4, p. 15–21, doi:10.1007/BF02380495.

Lucas, S.G., 1999, The epicontinental Triassic, an overview, *in* Bachmann, G.H., and Lerche, I., eds., Epicontinental Triassic International Symposium: Zentralblatt fur Geologie und Palaontologie Teil, v. 1, p. 475–496.

Lucas, S.G., 2010, The Triassic Timescale: Geological Society of London Special Publication 334, p. 103–118, doi:10.1144/SP334.1.

Lucas, S.G., and Orchard, M.J., 2004, Triassic, *in* Selley, R.C., Cocks, L.M.R., and Plimer, I.R., eds., Encyclopedia of Geology: Amsterdam, Elsevier, p. 344–351.

Maron, M., Rigo, M., Bertinelli, A., Katz, M.E., Godfrey, L., Zaffani, M., and Muttoni, G., 2015, Magnetostratigraphy, biostratigraphy and chemostratigraphy of the Pignola-Abriola section: New constraints for the Norian–Rhaetian boundary: Geological Society of America Bulletin, v. 127, p. 962–974, doi:10.1130/B31106.1.

Marzoli, A., Renne, P.R., Piccirillo, E.M., Ernesto, M., Bellieni, G., and De Min, A., 1999, Extensive 200-million-year-old continental flood basalts of the Central Atlantic Magmatic Province: Science, v. 284, p. 616–618, doi:10.1126/science.284.5414.616.

Marzoli, A., Bertrand, H., Knight, K.B., Cirilli, S., Buratti, N., Vérati, C., Nomade, S., Renne, P.R., Youbi, N., Martini, R., Allenbach, K., Neuwerth, R., Rapaille, C., Zaninetti, L., and Bellieni, G., 2004, Synchrony of the Central Atlantic magmatic province and the Triassic–Jurassic boundary climatic and biotic crisis: Geology, v. 32, p. 973–976, doi:10.1130/G20652.1.

Marzoli, A., Bertrand, H., Chiaradia, M., Fontignie, D., Youbi, N., and Bellieni, G., 2006a, The genesis of CAMP basalts (Morocco) from enriched lithosphere to late asthenosphere mantle sources: Geochimica et Cosmochimica Acta, v. 70, p. 396, doi:10.1016/j.gca.2006.06.799.

Marzoli, A., Rapaille, C., Reisberg, L., and Bertrand, H., 2006b, Trace element and Sr-Nd-Pb-Os evidence for a lithospheric mantle source for the European CAMP basalts: Geochimica et Cosmochimica Acta, v. 70, p. 397.

Mazza, M., Furin, S., Spötl, C., and Rigo, M., 2010, Generic turnovers of Carnian/Norian conodonts: Climatic control or competition?: Palaeogeography, Palaeoclimatology, Palaeoecology, v. 290, p. 120–137, doi:10.1016/j.palaeo.2009.07.006.

McElwain, J.C., Beerling, D.J., and Woodward, F.I., 1999, Fossil plants and global warming at the Triassic–Jurassic boundary: Science, v. 285, p. 1386–1390, doi:10.1126/science.285.5432.1386.

McRoberts, C.A., Krystyn, L., and Shea, A., 2008, Rhaetian (Late Triassic) Monotis (Bivalvia: Pectinoida) from the eastern Northern Calcareous Alps (Austria) and the end-Norian crisis in pelagic faunas: Palaeontology, v. 51, p. 721–735, doi:10.1111/j.1475-4983.2008.00776.x.

Meyers, P.A., 2014, Why are the $\delta^{13}C_{org}$ values in Phanerozoic black shales more negative than in modern marine organic matter?: Geochemistry, Geophysics, Geosystems, v. 15, p. 3085–3106, doi:10.1002/2014GC005305.

Miconnet, P., 1982, Precisions stratigraphiques et tectoniques dans un secteur du Lagonegro (Italie meridionale): Annales de la Societe Geologique du Nord, v. 102, p. 17–24.

Mortensen, J.K., and Hulbert, L.J., 1991, A U-Pb zircon age for a Maple Creek gabbro sill, Tatamagouche Creek area, southwest Yukon Territory: Radiogenic Age and Isotopic Studies, Report 5: Geological Survey of Canada, Paper 91-2, p. 175–179.

Mostardini, F., and Merlini, S., 1986, Appennino centro-meridionale. Sezioni geologiche e proposta di modello strutturale: Memorie della Societa Geologica Italiana, v. 35, p. 177–202.

Muttoni, G., Kent, D.V., Olsen, P., Di Stefano, P., Lowrie, W., Bernasconi, S., and Martin Hernandez, F., 2004, Tethyan magnetostratigraphy from Pizzo Mondello (Sicily) and correlation to the Late Triassic astrochronological polarity time scale: Geological Society of America Bulletin, v. 116, p. 1043–1058, doi:10.1130/B25326.1.

Muttoni, G., Kent, D.V., Jadoul, F., Olsen, P.E., Rigo, M., Galli, M.T., and Nicora, A., 2010, Rhaetian magneto-biostratigraphy from the Southern Alps (Italy): Constraints on Triassic chronology: Palaeogeography, Palaeoclimatology, Palaeoecology, v. 285, p. 1–16, doi:10.1016/j.palaeo.2009.10.014.

Muttoni, G., Mazza, M., Mosher, D., Katz, M.E., Kent, D.V., and Balini, M., 2014, A Middle–Late Triassic (Ladinian–Rhaetian) carbon and oxygen isotope record from the Tethyan Ocean: Palaeo-

geography, Palaeoclimatology, Palaeoecology, v. 399, p. 246–259, doi:10.1016/j.palaeo.2014.01.018.
Ogg, J.G., 2012, Triassic, *in* Gradstein, F.M., Ogg, J.G., Schmitz, M.D., and Ogg, G.M., eds., The Geologic Time Scale: Elsevier, p. 681–730, doi:10.1016/B978-0-444-59425-9.00025-1.
Orchard, M.J., 1991, Upper Triassic conodont biochronology and new index species from the Canadian Cordillera: Geological Survey of Canada Bulletin, v. 417, p. 299–335, doi:10.4095/132442.
Pálfy, J., and Kocsis, A.T., 2014, Volcanism of the Central Atlantic magmatic province as the trigger of environmental and biotic changes around the Triassic–Jurassic boundary, *in* Keller, G., and Kerr, A.C., eds., Volcanism, Impacts, and Mass Extinctions: Causes and Effect: Geological Society of America Special Paper 505, p. 245–261, doi:10.1130/2014.2505(12).
Pálfy, J., Demeny, A., Haas, J., Hetenyi, M., Orchard, M.J., and Veto, I., 2001, Carbon isotope anomaly and other geochemical changes at the Triassic–Jurassic boundary from a marine section in Hungary: Geology, v. 29, p. 1047–1050, doi:10.1130/0091-7613(2001)029<1047:CIAAOG>2.0.CO;2.
Pálfy, J., Demeny, A., Haas, J., Carter, E.S., Gorog, A., Halasz, D., Oravecz-Scheffer, A., Hetenyi, M., Marton, E., Orchard, M.J., Ozsvart, P., Veto, I., and Zaizon, N., 2007, Triassic–Jurassic boundary events inferred from integrated stratigraphy of the Csovar section, Hungary: Palaeogeography, Palaeoclimatology, Palaeoecology, v. 244, p. 11–33, doi:10.1016/j.palaeo.2006.06.021.
Pallister, J.S., Budahn, J.R., and Murchey, B.L., 1989, Pillow basalts of the Angayucham Terrane: Oceanic Plateau and Island Crust Accreted to the Brooks Range: Journal of Geophysical Research, v. 94, p. 15901–15923, doi:10.1029/JB094iB11p15901.
Palmer, M.R., and Elderfield, H., 1985, Sr isotope composition of sea water over the past 75 Myr: Nature, v. 314, p. 526–528, doi:10.1038/314526a0.
Palmer, M.R., and Edmond, J.M., 1989, The Strontium Isotope Budget of the Modern Ocean: Earth and Planetary Science Letters, v. 92, no. 1, p. 11–26, doi:10.1016/0012-821X(89)90017-4.
Passeri, L., Bertinelli, A., and Ciarapica, G., 2005, Palaeogeographic meaning of the late Triassic–Early Jurassic Lagonegro units: Bollettino della Società Geologica Italiana, v. 124, p. 231–245.
Payne, J.L., and Kump, L.R., 2007, Evidence for recurrent Early Triassic massive volcanism from quantitative interpretation of carbon isotope fluctuations: Earth and Planetary Science Letters, v. 257, p. 264-277, doi:10.1016/j.epsl.2007.01.034.
Payne, J.L., Lehrmann, D.J., Wei, J., Orchard, M.J., Schrag, D.P., and Knoll, A.H., 2004, Large perturbations of the carbon cycle during recovery from the end-Permian extinction: Nature, v. 305, p. 506–509.
Peucker-Ehrenbrink, B., and Ravizza, G., 2000, The marine osmium isotope record: Terra Nova, v. 12, 5, p. 205–219, doi:10.1046/j.1365-3121.2000.00295.x.
Pogge von Strandmann, P.A.E., Jenkyns, H.C., and Woodfine, R.G., 2013, Lithium isotope evidence for enhanced weathering during Oceanic Anoxic Event 2: Nature Geoscience, v. 6, no. 8, p. 668–672, doi:10.1038/ngeo1875.
Preto, N., Kustatscher, E., and Wignall, P.B., 2010, Triassic climates—State of the art and perspectives: Palaeogeography, Palaeoclimatology, Palaeoecology, v. 290, p. 1–10, doi:10.1016/j.palaeo.2010.03.015.
Preto, N., Rigo, M., Agnini, C., Bertinelli, A., Guaiumi, C., Borello, S., and Westphal, H., 2012, Triassic and Jurassic calcareous nannofossils of the Pizzo Mondello section: A SEM study: Rivista Italiana di Paleontologia e Stratigrafia, v. 118, no. 1, p. 131–141.
Preto, N., Agnini, C., Rigo, M., Sprovieri, M., and Westphal, H., 2013, The calcareous nannofossil Prinsiosphaera achieved rock-forming abundances in the latest Triassic of western Tethys: Consequences for the $\delta^{13}C$ of bulk carbonate: Biogeosciences, v. 10, p. 6053–6068, doi:10.5194/bg-10-6053-2013.
Prokoph, A., El Bilali, H., and Ernst, R., 2013, Periodicities in the emplacement of large igneous provinces through the Phanerozoic: Relations to ocean chemistry and marine biodiversity evolution: Geoscience Frontiers, v. 4, p. 263–276, doi:10.1016/j.gsf.2012.08.001.
Ramezani, J., Bowring, S.A., Pringle, M.S., Winslow, F.D., III, and Rasbury, E.T., 2005, The Manicouagan impact melt rock: A proposed standard for the intercalibration of U-Pb and $^{40}Ar/^{39}Ar$ isotopic systems: Geochimica et Cosmochimica Acta, v. 69, Suppl., p. A321.
Ramezani, J., Hoke, G.D., Fastovsky, D.E., Bowring, S.A., Therrien, F., Dworkin, S.I., Atchley, S.C., and Nordt, L.C., 2011, High precision U-Pb zircon geochronology of the Late Triassic Chinle Formation, Petrified Forest National Park (Arizona, USA): Temporal constraints on the early evolution of dinosaurs: Geological Society of America Bulletin, v. 123, p. 2142–2159, doi:10.1130/B30433.1.
Rampino, M.R., and Stothers, R.B., 1988, Flood basalt volcanism during the past 250 million years: Science, v. 241, p. 663–668, doi:10.1126/science.241.4866.663.
Raup, D.M., and Sepkoski, J.J., 1982, Mass extinction in the fossil record: Science, v. 215, p. 1501–1503, doi:10.1126/science.215.4539.1501.
Ravizza, G.E., and Peucker-Ehrenbrink, B, 2003, The marine $^{187}Os/^{188}Os$ record of the Eocene-Oligocene transition: The interplay of weathering and glaciation: Earth and Planetary Science Letters, v. 210, p. 151–165, doi:10.1016/S0012-821X(03)00137-7.
Raymo, M.E., Ruddiman, W.F., and Froelich, P.N., 1988, Influence of late Cenozoic mountain building on ocean geochemical cycles: Geology, v. 16, p. 649–653, doi:10.1130/0091-7613(1988)016<0649:IOLCMB>2.3.CO;2.
Reggiani, L., Bertinelli, A., Ciarapica, G., Marcucci, M., Passeri, L., Ricci, C., and Rigo, M., 2005, Triassic–Jurassic stratigraphy of the Madonna del Sirino succession (Lagonegro basin, Southern Apennines, Italy): Bollettino della Società Geologica Italiana, v. 124, p. 281–291.
Richoz, S., Krystyn, L., and Spotl, C., 2007, Towards a carbon isotope reference curve of the Upper Triassic: New Mexico Museum of Natural History and Science Bulletin, v. 41, p. 366–367.
Rigo, M., and Joachimski, M.M., 2010, Palaeoecology of Late Triassic conodonts: Constraints from oxygen isotopes in biogenic apatite: Acta Palaeontologica Polonica, v. 55, no. 3, p. 471–478, doi:10.4202/app.2009.0100.
Rigo, M., De Zanche, V., Mietto, P., Preto, N., and Roghi, G., 2005, Biostratigraphy of the Calcari con Selce formation: Bollettino della Società Geologica Italiana, v. 124, p. 293–300.
Rigo, M., Preto, N., Roghi, G., Tateo, F., and Mietto, P., 2007, A rise in the Carbonate Compensation Depth of western Tethys in the Carnian (Late Triassic): Deep-water evidence for the Carnian Pluvial Event: Palaeogeography, Palaeoclimatology, Palaeoecology, v. 246, p. 188–205, doi:10.1016/j.palaeo.2006.09.013.
Rigo, M., Preto, N., Franceschi, M., and Guaiumi, C., 2012a, Stratigraphy of the Carnian-Norian Calcari con Selce Formation in the Lagonegro Basin, Southern Apennines: Rivista Italiana di Paleontologia e Stratigrafia, v. 118, p. 143–154.
Rigo, M., Trotter, J.A., Preto, N., and Williams, I.S., 2012b, Oxygen isotopic evidence for Late Triassic monsoonal upwelling in the northwestern Tethys: Geology, v. 40, no. 6, p. 515–518, doi:10.1130/G32792.1.
Rigo, M., Bertinelli, A., Concheri, G., Gattolin, G., Godfrey, L., Katz, M.E., Maron, M., Muttoni, G., Sprovieri, M., Stellin, F., and Zaffani, M., 2016, The Pignola-Abriola section (southern Apennines, Italy): A new GSSP candidate for the base of the Rhaetian Stage: Lethaia, v. 49, p. 287–306, doi:10.1111/let.12145.
Ruffell, A., Simms, M.J., and Wignall, P.B., 2015, The Carnian Humid Episode of the Late Triassic: A Review: Geological Magazine, v. 153, no. 2, p. 271–284, doi:10.1017/S0016756815000424.
Ruhl, M., and Kurschner, W.M., 2011, Multiple phases of carbon cycle disturbance from large igneous province formation at the Triassic–Jurassic transition: Geology, v. 39, p. 431–434, doi:10.1130/G31680.1.
Saunders, A.D., Fitton, J.G., Kerr, A.C., Norry, M.J., and Kent, R.W., 1997, The North Atlantic Igneous Province, *in* Mahoney, J.J., and Coffin, M.F., eds., Large Igneous Provinces: Continental, Oceanic, and Planetary Flood Volcanism: American Geophysical Union Geophysical Monograph, v. 100, p. 45–93, doi:10.1029/GM100p0045.
Scandone, P., 1967, Studi di geologia lucana: La serie calcareo-silicomarnosa: Bollettino Società Naturalisti Napoli, v. 76, p. 1–175.
Schaller, M.F., Wright, J.D., Kent, D.V., and Olsen, P.E., 2012, Rapid emplacement of the Central Atlantic Magmatic Province as a net sink for CO_2: Earth and Planetary Science Letters, v. 323–324, p. 27–39, doi:10.1016/j.epsl.2011.12.028.
Schaller, M.F., Fung, M.K., Wright, J.D., Katz, M.E., and Kent, D.V., 2016, Impact ejecta at the Paleocene–Eocene boundary: Science, v. 354, no. 6309, p. 225–229, doi:10.1126/science.aaf5466.
Schmincke, H.-U., 2004, Volcanism: Berlin, Heidelberg, Springer-Verlag, 364 p, doi:10.1007/978-3-642-18952-4.
Schoene, B., Guex, J., Bartolini, A., Schaltegger, U., and Blackburn, T.J., 2010, A correlation between the Triassic–Jurassic boundary mass extinction and flood basalt eruption at the 100-ka level using ID-TIMS U/Pb zircon geochronology: Geology, v. 38, p. 387–390, doi:10.1130/G30683.1.
Self, S., Thordarson, T., and Widdowson, M., 2005, Gas fluxes from flood basalt eruptions: Elements, v. 1, p. 283–287, doi:10.2113/gselements.1.5.283.
Sell, B., Ovtcharova, M., Guex, J., Bartolini, A., Jourdan, F., Spangenberg, J.E., Vicente, J.C., and Schaltegger, U., 2014, Evaluating the temporal link between the Karoo LIP and climatic-biologic events of the Toarcian Stage with high-precision U-Pb geochronology: Earth and Planetary Science Letters, v. 408, p. 48–56, doi:10.1016/j.epsl.2014.10.008.
Selli, R., 1962, Il Paleogene nel quadro della Geologia dell'Italia Meridionale: Memorie della Societa Geologica Italiana, v. 3, p. 737–790.

Şengör, A.M.C., Yilmaz, Y., and Sungurlu, O., 1984, Tectonics of the Mediterranean Cimmerides: Nature and evolution of the western termination of Palaeo-Tethys: Geological Society of London, Special Publications, v. 17, p. 77–112, doi:10.1144/GSL.SP.1984.017.01.04.

Sephton, M.A., Amor, K., Franchi, I.A., Wignall, P.B., Newton, R., and Zonneveld, J.P., 2002, Carbon and nitrogen isotope disturbances and an end-Norian (Late Triassic) extinction event: Geology, v. 30, p. 1119–1122, doi:10.1130/0091-7613(2002)030<1119:CANIDA>2.0.CO;2.

Shirey, S.B., and Walker, R.J., 1998, The Re-Os isotope system in cosmochemistry and high-temperature geochemistry: Annual Review of Earth and Planetary Sciences, v. 26, p. 423–500, doi:10.1146/annurev.earth.26.1.423.

Simms, M.J., and Ruffell, A.H., 1989, Synchroneity of climatic change and extinctions in the Late Triassic: Geology, v. 17, p. 265–268, doi:10.1130/0091-7613(1989)017<0265:SOCCAE>2.3.CO;2.

Simms, M.J., and Ruffell, A.H., 1990, Climatic and biotic change in the late Triassic: Journal of the Geological Society of London, v. 147, p. 321–327, doi:10.1144/gsjgs.147.2.0321.

Simms, M.J., Ruffell, A.H., and Johnson, A.L.A., 1995, Biotic and climatic changes in the Carnian (Triassic) of Europe and adjacent areas, *in* Fraser, N.C., and Sues, H.D., eds., In the Shadow of the Dinosaurs: Early Mesozoic Tetrapods: Cambridge University Press, p. 352–365.

Sobolev, S.V., Sobolev, A.V., Kuzmin, D.V., Krivolutskaya, N.A., Petrunin, A.G., Arndt, N.T., Radko, V.A., and Vasiliev, Y.R., 2011, Linking mantle plumes, large igneous provinces and environmental catastrophes: Nature, v. 477, p. 312–316, doi:10.1038/nature10385.

Speranza, F., Minelli, L., Pignatelli, A., and Chiappini, M., 2012, The Ionian Sea: The oldest in situ ocean fragment of the world?: Journal of Geophysical Research, v. 117, B12101, doi:10.1029/2012JB009475.

Stampfli, G., Marcoux, J., and Baud, A., 1991, Tethyan margins in space and time: Palaeogeography, Palaeoclimatology, Palaeoecology, v. 87, p. 373–409, doi:10.1016/0031-0182(91)90142-E.

Stampfli, G.M., and Marchant, R.H., 1995, Plate configuration and kinematics in the Alpine region: Accademia Nazionale Delle Scienze: Scritti e Documenti, v. 14, p. 147–166.

Stampfli, G.M., Mosar, J., De Bono, A., and Vavassis, I., 1998, Late Paleozoic, early Mesozoic plate tectonics of the western Tethys: Bulletin of the Geological Society of Greece, v. 32, p. 113–120.

Stampfli, G.M., Vavassis, I., De Bono, A., Rosselet, F., Matti, B., and Bellini, M., 2003, Remnants of the Paleotethys oceanic suture-zone in the western Tethys area: Bollettino della Società Geologica Italiana, Special Volume, no. 2, p. 1–23.

Sussman, A.J., and Weil, A.B., eds., 2004, Orogenic Curvature: Integrating Paleomagnetic and Structural Analyses: Geological Society of America Special Paper 383, 271 p.

Swart, P.K., 2008, Global synchronous changes in the carbon isotopic composition of carbonate sediments unrelated to changes in the global carbon cycle: Proceedings of the National Academy of Sciences of the United States of America, v. 105, no. 37, p. 13,741–13,745, doi:10.1073/pnas.0802841105.

Swart, P.K., and Eberli, G.P., 2005, The nature of the $\delta^{13}C$ of periplatform sediments: Implications for stratigraphy and the global carbon cycle: Sedimentary Geology, v. 175, p. 115–129, doi:10.1016/j.sedgeo.2004.12.029.

Symonds, R.B., Rose, W.I., Bluth, G., and Gerlach, T.M., 1994, Volcanic gas studies: Methods, results, and applications, *in* Carroll, M.R., and Holloway, J.R., eds., Volatiles in Magmas: Mineralogical Society of America Reviews in Mineralogy 30, p. 1–66.

Tanner, L.H., 2010, The Triassic isotope record, *in* Lucas, S.G., ed., The Triassic Timescale: Geological Society London Special Publication 334, p. 103–118.

Tanner, L.H., and Lucas, S.G., 2016, Stratigraphic distribution and significance of a 15 million-year record of fusain in the Upper Triassic Chinle Group, southwestern USA: Palaeogeography, Palaeoclimatology, Palaeoecology, doi:10.1016/j.palaeo.2016.08.034.

Tanner, L.H., Lucas, S.G., and Chapman, M.G., 2004, Assessing the record and causes of Late Triassic extinction: Earth-Science Reviews, v. 65, p. 103–139, doi:10.1016/S0012-8252(03)00082-5.

Tanner, L.H., Schiattarella, M., and Di Leo, P., 2006, Carbon isotope record of Upper Triassic strata of the Lagonegro Basin, Southern Apennines, Italy: Preliminary results: Mexico Museum of Natural History and Science Bulletin, v. 37, p. 23–28.

Tanner, L.H., Ciarapica, G., Reggiani, L., and Atudorei, V., 2007, Upper Triassic carbon isotope stratigraphy of the Lagonegro Succession, Southern Apennines, Italy: New Mexico Natural History and Science Bulletin, v. 41, p. 406–410.

Taylor, A.S., and Lasaga, A.C., 1999, The role of basalt weathering in the Sr isotope budget of the oceans: Chemical Geology, v. 161, no. 1–3, p. 199–214, doi:10.1016/S0009-2541(99)00087-X.

Tejada, M.L.G., Suzuki, K., Kuroda, J., Coccioni, R., Mahoney, J.J., Ohkouchi, N., Sakamoto, T., and Tatsumi, Y., 2009, Ontong Java Plateau eruption as a trigger for the early Aptian oceanic anoxic event: Geology, v. 37, p. 855–858, doi:10.1130/G25763A.1.

Tolan, T.L., Reidel, S.P., Beeson, M.H., Anderson, J.L., Fecht, K.R., and Swanson, D.A., 1989, Revisions to the estimates of the areal extent and volume of the Columbia River Basalt Group, *in* Reidel, S.P., and Hooper, P.R., eds., Volcanism and Tectonism in the Columbia River Flood-Basalt Province: Geological Society of America Special Paper 239, p. 1–20, doi:10.1130/SPE239-p1.

Trotter, A.J., Williams, S.I., Nicora, A., Mazza, M., and Rigo, M., 2015, Long-term cycles of Triassic climate change: A new $\delta^{18}O$ record from conodont apatite: Earth and Planetary Science Letters, v. 415, p. 165–174, doi:10.1016/j.epsl.2015.01.038.

Turgeon, S.C., and Creaser, R.A., 2008, Cretaceous oceanic anoxic event 2 triggered by a massive magmatic episode: Nature, v. 454, p. 323–326, doi:10.1038/nature07076.

van de Schootbrugge, B., Payne, J.L., Tomasovych, A., Pross, J., Fiebig, J., Benbrahim, M., Follmi, K.B., and Quan, T.M., 2008, Carbon cycle perturbation and stabilization in the wake of the Triassic–Jurassic boundary mass extinction event: Geochemistry, Geophysics, Geosystems, v. 9, Q04028, doi:10.1029/2007GC001914.

Veizer, J., Buhl, D., Diener, A., Ebneth, S., Podlaha, O.G., Bruckschen, P., Jasper, T., Korte, C., Schaaf, M., Ala, D., and Azmy, K., 1997, Strontium isotope stratigraphy: Potential resolution and event correlation: Paleogeography, Paleoclimatology, Paleoecology, v. 132, p. 65–77, doi:10.1016/S0031-0182(97)00054-0.

Veizer, J., Ala, K., Azmy, K., Bruckschen, P., Buhl, D., Bruhn, F., Carden, G.A.F., Diener, A., Ebneth, S., Godderis, Y., Jasper, T., Korte, C., Pawellek, F., Podlaha, O.G., and Strauss, H., 1999, $^{87}Sr/^{86}Sr$, $\delta^{13}C$ and $\delta^{18}O$ evolution of Phanerozoic seawater: Chemical Geology, v. 161, p. 59–88, doi:10.1016/S0009-2541(99)00081-9.

Ward, P.D., Garrison, G.H., Haggart, J.W., Kring, D.A., and Beattie, M.J., 2004, Isotopic evidence bearing on Late Triassic extinction events, Queen Charlotte Islands, British Columbia, and implications for the duration and cause of the Triassic/Jurassic mass extinction: Earth and Planetary Science Letters, v. 224, p. 589–600, doi:10.1016/j.epsl.2004.04.034.

Whiteside, J.H., and Ward, P.D., 2011, Ammonoid diversity and disparity track episodes of chaotic carbon cycling during the early Mesozoic: Geology, v. 39, p. 99–102, doi:10.1130/G31401.1.

Whiteside, J.H., Olsen, P.E., Eglinton, T., Brookfield, M.E., and Sambrotto, R.N., 2010, Compound-specific carbon isotopes from Earth's largest flood basalt eruptions directly linked to the end-Triassic mass extinction: Proceedings of the National Academy of Sciences of the United States of America, v. 107, p. 6721–6725, doi:10.1073/pnas.1001706107.

Wignall, P.B., 2001, Large igneous provinces and mass extinctions: Earth-Science Reviews, v. 53, p. 1–33, doi:10.1016/S0012-8252(00)00037-4.

Wignall, P.B., Zonneveld, J.-P., Newton, R.J., Amor, K., Sephton, M.A., and Hartley, S., 2007, The end Triassic mass extinction record of Williston Lake, British Columbia: Palaeogeography, Palaeoclimatology, Palaeoecology, v. 253, p. 385–406, doi:10.1016/j.palaeo.2007.06.020.